ECMWF COPERNICUS REPORT

Copernicus Atmosphere Monitoring Service

Regional Production, Updated documentation covering all Regional operational systems and the ENSEMBLE

Following U2 upgrade, February 2020

Issued by: METEO-FRANCE / G. Collin

Date: 05/03/2020

Ref:

CAMS50_2018SC2_D2.0.2-U2_Models_documentation_202003_v2

Table of Contents

Executive summary

The Copernicus Atmosphere Monitoring Service (CAMS, atmosphere.copernicus.eu/) is establishing the core global and regional atmospheric environmental service delivered as a component of Europe's Copernicus programme. The Regional forecasting service (CAMS_50) currently provides daily 4-day forecasts of the main air quality species and analyses of the day before, as well as posteriori re-analyses using the latest validated observation dataset available for assimilation. Since the U1 upgrade performed in summer 2019, 9 state-of-the-art atmospheric chemistry models take part in the operation production. A median ENSEMBLE is calculated from the 9 model outputs, since ensemble products generally yield better performance than the individual model products.

Following the U2 upgrade of February 2020, this document provides an updated description of the 9 operational models contributing to the ENSEMBLE, and also the method used for the ENSEMBLE production. For each system, the main components of the model are specified: chemistry schemes, aerosol representation, emissions and deposition, resolved and sub-grid transport, boundary conditions, assimilation system. The document is helpful to identify the differences and common features between the models. It may be used as a reference information regarding the CAMS Regional operational production.

1. ENSEMBLE factsheet

1.1 Assimilation and forecast system: synthesis of the main characteristics

ENSEMBLE forecasts and analyses	
Horizontal resolution	0.1° regular lat-lon grid
Domain	25°W-45°E, 30°N-72°N
ENSEMBLE method	Median model: for each grid-cell, the value corresponds to the median of the different model values
Individual models	CHIMERE, EMEP, EURAD-IM, LOTOS-EUROS, MATCH, MOCAGE, SILAM Since Oct. 2019: DEHM, GEM-AQ

1.2 ENSEMBLE background information

Based on a sample of individual model members, the ensemble approach is useful and relevant for air quality monitoring (Galmarini et al, 2004). The ensemble products, indeed, generally yield better performance than the individual model products. Besides, the spread between the different members may be used to provide some information about the uncertainty of the ensemble products. Consequently, the forecasts, analyses and re-analyses delivered as part of the CAMS Regional production are based on an ensemble approach.

1.2.1 Method

The ENSEMBLE is currently based upon a median value approach (Marécal et al, 2015).

For each time step of the daily forecasts, the different individual model fields (see 1.2.2) are interpolated on a common regular 0.1°x0.1° grid over the European domain (25°W-45°E, 30°N-72°N) used for the CAMS Regional production. For each point of this grid, the ENSEMBLE model value is simply defined as the median value of all the individual models' forecasts on this point. The median is defined as the value having 50% of individual models with higher values and 50% with lower values.

This method provides an optimal estimate in the statistical sense (Riccio et al, 2007) and is rather insensitive to outliers in the forecasts, which is a useful property for the quality and for the reliability of the CAMS Regional production. The method is also little sensitive if a particular model forecast is occasionally missing.

1.2.2 Individual models

The ENSEMBLE production is based on the 9 individual models listed in Table 1.

Table 1. Individual models contributing to the ENSEMBLE

Model names	**Institutes**
CHIMERE	INERIS (France)
EMEP	MET Norway (Norway)
EURAD-IM	FZJ-IEK8 (Germany)
LOTOS-EUROS	KNMI, TNO (The Netherlands)
MATCH	SMHI (Sweden)
MOCAGE	Meteo-France (France)
SILAM	FMI (Finland)
DEHM	AARHUS UNIVERSITY (Denmark)
GEM-AQ	IEP-NRI (Poland)

DEHM and GEM-AQ take part in operational production since the U1.2 upgrade of 16/10/2019. In addition, 2 candidate models will be evaluated over the course of CAMS_50.II for a possible future integration in the ENSEMBLE: MINNI (ENEA, Italy) and MONARCH (BSC, Spain).

The main characteristics of the individual models are outlined in half-yearly development reports, as well as in the present document that is regularly updated and available from the CAMS website[1]. The latter also provides access to quarterly NRT production reports[2] comprising, per model, a description of the daily analysis and forecast activities undertaken by the models and a performance review.

1.2.3 Common input forcing

All the regional chemistry-transport models share common inputs regarding meteorology, boundary conditions and emissions. Some specificities in the implementation of individual model are highlighted in the following sections.

Using common anthropogenic emission is a very strong requirement in the CAMS_50 setup. As of U2, the reference emission dataset is CAMS-REG-AP_v3.1/2016 provided by CAMS_81. We also implemented two new PM tracers helping in the identification of anthropogenic activities leading to air quality episodes. Those tracers correspond to Elemental Carbon in the $PM_{2.5}$ fraction, depending on the emission source: fossil fuel (EC_ff) or wood burning (EC_wb).

[1] https://atmosphere.copernicus.eu/documentation-regional-systems
[2] https://atmosphere.copernicus.eu/validation-regional-systems

The emissions of EC_ff and EC_wb are estimated using information for each country and activity provided by CAMS_81: (i) the share of biomass in total $PM_{2.5}$ emissions, and the composition of $PM_{2.5}$ (in particular EC/OC share). These factors are then applied to the total $PM_{2.5}$ emissions by gridpoint for each model to derive EC_ff and EC_wb emissions.

A major issue lies however in the fact that wood burning emission reporting is far from being harmonised in the official EMEP inventories underlying the national totals in CAMS-REG-AP_v3.1. This is due to a different interpretation of EMEP States Parties on whether only the filterable fraction should be reported, or if the condensable part should also be accounted for. The issue has been documented in (Denier van der Gon et al., 2015) and it is also a focus on intense recent development under the CLRTAP convention (TFEIP/TFMM, 2018;EMEP, 2019). CAMS_50 will be following closely these developments to improve the reliability of EC_wb modelling.

Using common wildfire emission is also a strong requirement. At present we use hourly GFAS provided by ECMWF in pre-operational stream. Injection heights information is not available in these hourly emission (whereas it was provided in the daily operational stream). As of U2, we implemented a new aerosol tracer (PM_wilffire) corresponding to the species tpmfire in the GFAS emissions.

1.2.4 Air quality NRT EPSgrams

Daily, “EPSgrams” for 67 major European cities and urban areas are produced and displayed on the CAMS website for Regional Air Quality. Such graphics are common for presenting ensemble meteorological forecast products but, to our knowledge, this is the first experimental implementation worldwide in the field of Air Quality, which started within the GEMS project.

Figure 1 presents an example of AQ EPSgram. For the 4 main pollutants (ozone, NO_2, SO_2 and PM_{10}) forecasts are plotted every 3 hours as bars, which indicate the range of forecasts of individual ensemble members (minimum, maximum and percentiles 10, 25, 50, 75 and 90). This presentation allows users to assess the dispersion within the ensemble for each species and each 3-hourly forecast horizon at the given location of the EPSgram.

The 67 selected sites include the 41 European capitals and 26 urban areas that are among the most populated ones and where pollution episodes are common. The forecasts are based upon models that have resolutions of ~10km to 25km, which is too coarse to account for very local and urban effects (high primary pollutants, titration of ozone, etc.). The AQ EPSgrams presented have thus to be taken with caution; the forecast does not correspond to city centre values, but rather to values representative of the background in the urban area around the city.

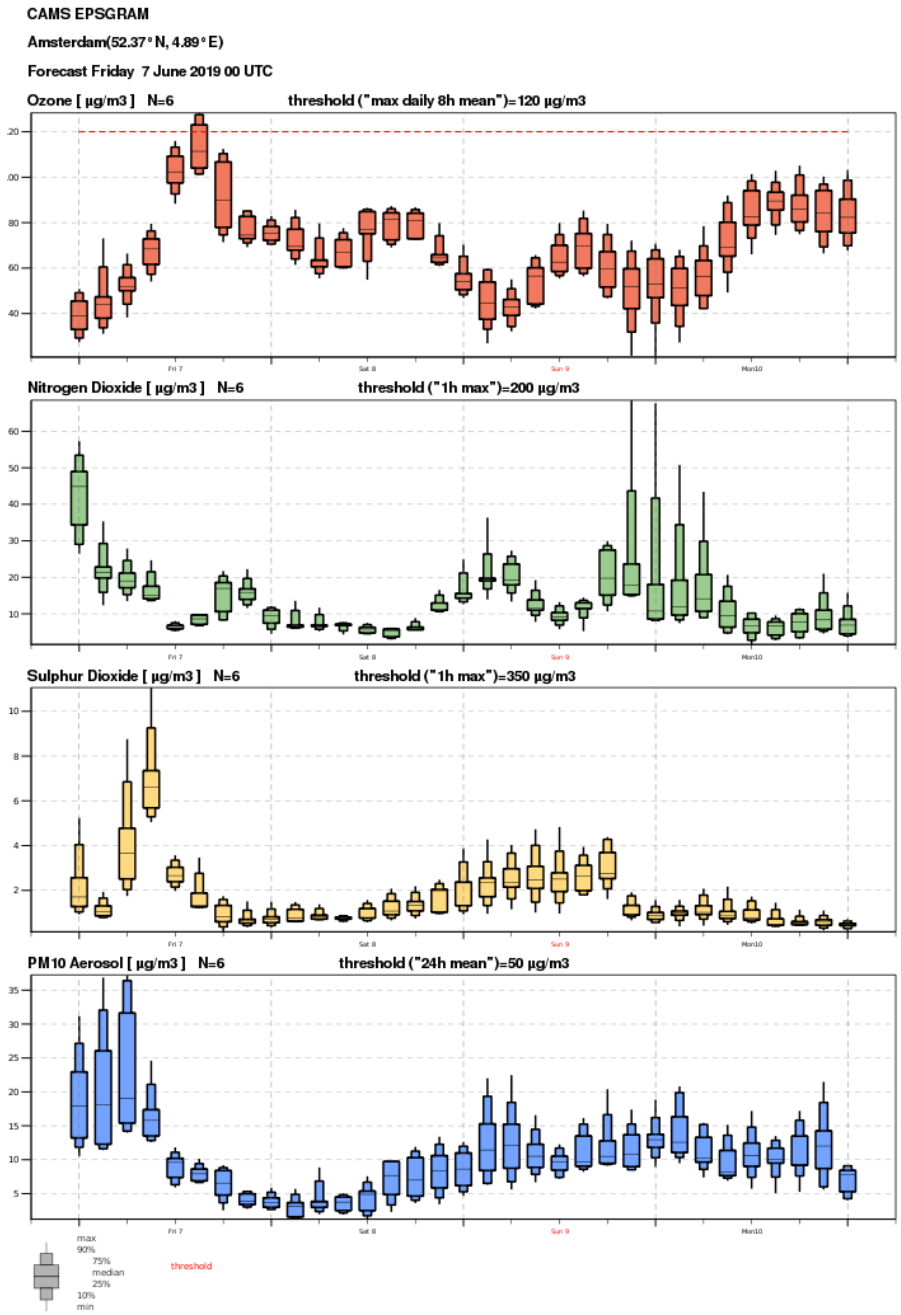

Figure 1 - Example of air quality EPSgram at the location of the city of Amsterdam (the Netherlands), concerning June 7th, 2019.

2. CHIMERE factsheet

2.1 Assimilation and forecast system: synthesis of the main characteristics

Assimilation and forecast system	
Horizontal resolution	0.1°x0.1°
Vertical resolution	Variable, 9 levels from the surface up to 500 hPa; 7 levels below 2 km
Gas phase chemistry	MELCHIOR2, comprising 44 species and 120 reactions (Derognat, 2003)
Heterogeneous chemistry	NO_2, HNO_3, N_2O_5
Aerosol size distribution	10 bins from 10 nm to 40 µm
Inorganic aerosols	Primary particle material, nitrate, sulphate, ammonium
Secondary organic aerosols	Biogenic, anthropogenic
Aqueous phase chemistry	Sulphate
Dry deposition/sedimentation	Classical resistance approach
Mineral dust	Dusts are considered coming from BC and emitted by desert area inside the domain
Sea Salt	Inert sea salt
Boundary values	Values provided by CAMS global
Initial values	24h forecast from the day before
Anthropogenic emissions	CAMS-REG-AP_v3.1/2016
Biogenic emissions	MEGAN
Forecast system	
Meteorological driver	00:00 UTC operational IFS forecast from the day before
Assimilation system	
Assimilation method	Kriging-based analysis
Observations	Surface ozone, NO_2, PM_{10} and $PM_{2.5}$
Frequency of assimilation	Every hour over the day before
Meteorological driver	00:00 UTC operational IFS forecast for the day before

2.2 Forward model

The CHIMERE multi-scale model is primarily designed to produce daily forecasts of ozone, aerosols and other pollutants, and to make long-term simulations for emission control scenarios. CHIMERE runs over a range of spatial scale from the regional scale (several thousand kilometres) to the urban

scale (100-200 Km), with resolutions from 1-2 Km to 100 Km. The chemical mechanism (MELCHIOR) is adapted from the original EMEP mechanism. Photolytic rates are attenuated using liquid water or relative humidity. Boundary layer turbulence is represented as a diffusion (Troen and Mahrt, 1986, BLM). Vertical wind is diagnosed through a bottom-up mass balance scheme. Dry deposition is as in Wesely (1989). Wet deposition is included. 6 aerosol sizes are represented as bins in the model. Aerosol thermodynamic equilibrium is achieved using the ISORROPIA model. Several aqueous-phase reactions are considered. Secondary organic aerosols formations are considered. Advection is performed by the PPM (Piecewise Parabolic Method) 3d order scheme for slow species. The numerical time solver is the TWOSTEP method. Its use is relatively simple, provided input data is correctly supplied. It can be run with several vertical resolutions, and with a wide range of complexity. It can be run with several chemical mechanisms, simplified or more complete, with or without aerosols.

2.2.1 Model geometry

CHIMERE is a Eulerian deterministic model, using variable resolution in time and space (for Cartesian grids).

The model uses any number of vertical layers, described in hybrid sigma-p coordinates. The model runs over the CAMS domain with a 0.1°x0.1° resolution and 9 vertical levels, extending from the surface up to 500 hPa.

2.2.2 Forcings and boundary conditions

2.2.2.1 Meteorology

Within CAMS, CHIMERE is directly forced by the IFS forecasts from the daily operational products delivered at 00 UTC.

2.2.2.2 Chemistry

Boundary conditions can be either "external", or given by a coarse resolution CHIMERE simulation.

The CAMS regional forecasts of CHIMERE use the global CAMS production forcing from C-IFS (see Table 2). In case the production is delayed, a back-up forcing is available with a climatology built on 5 years of the MACC/CAMS re-analysis.

Use of Sea Salt boundary conditions was suspended in the past due to high overestimation. The corrective approach will be implemented before the end of 2019.

Table 2. The chemical and aerosol species taken from C-IFS and used in CHIMERE

C-IFS Species	**Coupled to CHIMERE Species**
SO_4 (0.06-1.0)	H_2SO_4 (bins 3-4-5-6)
OM (0.06-1.0)	AnBmP BiA1D BiBmP (bins 3-4-5-6)
BC (0.06-1.0)	BCAR (bins 3-4-5-6)
OM (0.06-1.0)	OCAR (bins 3-4-5-6)
DUST1 (0.06-1.1)	DUST (bins 3-4-5-6)
DUST2 (1.1-1.8)	DUST (bin 7)
DUST3 (1.8-40)	DUST (bins 7-8-9-10)
C_2H_6	C_2H_6
CH_2O	HCHO
CH_4	CH_4
CO	CO
HNO_3	HNO_3
ISOP	C_5H_8
NO_2	NO_2
GO_3	O_3
PAN	PAN
SO_2	SO_2

2.2.2.3 Land use

The proposed domain interface is based on the Global Land Cover Facility (GLCF): http://glcf.umiacs.umd.edu/data/landcover 1kmx1km resolution database from the University of Maryland, following the methodology of Hansen et al. (2000, J. Remote Sensing).

2.2.2.4 Surface emissions

The surface emissions are from the TNO emission inventory for anthropogenic emissions. Biogenic emissions are calculated online with the MEGAN module.
Hourly GFAS Fire emissions are downloaded daily from the dedicated Copernicus service through the MARS interface, use of ECPDS is under investigation.
Dust emissions are calculated online within CHIMERE.

2.2.3 Dynamical core

3 advection schemes are implemented: the Parabolic Piecewise Method (PPM, a 3-order horizontal scheme, after Colella and Woodward, 1984), the Godunov scheme (Van Leer, 1979) and the simple upwind first-order scheme.

2.2.4 Physical parameterisations

2.2.4.1 Turbulence and convection

Vertical turbulent mixing takes place only in the boundary layer. The formulation uses K-diffusion following the parameterisation of [Troen and Mahrt, 1986], without counter-gradient term.

2.2.4.2 Deposition

Dry deposition is considered for model gas species i and is parameterised as a downward flux F(d,i)= -v(d,i) c(i) out of the lowest model layer with c(i) being the concentration of species i. As commonly, the deposition velocity is described through a resistance analogy [Wesely, 1989]. The wet deposition follows the scheme proposed by [Loosmore, 2004].

2.2.5 Chemistry and aerosols

In order to decrease the computing time, a reduced mechanism with 44 species and about 120 reactions is derived from MELCHIOR [Derognat, 2003], following the concept of chemical operators [Carter, 1990]. This reduced mechanism is called MELCHIOR2 hereafter.

The CAMS CHIMERE version consists in the baseline gas-phase version with MELCHIOR2 chemistry, together with a sectional aerosol module. This module accounts for 7 species (primary particle material, nitrate, sulfate, ammonium, biogenic secondary organic aerosol SOA, anthropogenic SOA and water). Potentially, chloride and sodium can be included (high computing time). The aerosol distribution is represented using 9 bins from 10 nm to 10 µm.

2.3 Assimilation system

The CHIMERE assimilation for CAMS relies on a kriging based-approach to assimilate hourly concentration values for correcting the raw forecasts. This method has been widely evaluated and validated in the PREV'AIR (Rouïl et al, 2005) system for ozone and PM_{10}. However, future evolution of the CHIMERE assimilation system is foreseen to perform multi-pollutant and multi-sensor assimilation at the same time with a more complex method.

2.3.1 Kriging-based analysis

Several variants of kriging have been tested and compared (Malherbe et al., 2012): kriging of the innovations (i.e. kriging of CHIMERE errors); kriging with CHIMERE as external drift; ordinary co-kriging between the observations and CHIMERE.

- For operational applications, kriging with external drift, which gave the highest scores for ozone (Malherbe and Ung, 2009) and is faster than co-kriging, was found to be the best compromise between efficiency and computing time. It has been implemented in PREV'AIR since 2010, as replacement for kriging of the innovations. It proceeds according to the following steps:

Hourly monitoring data are retrieved from CAMS_50. Linear regression between a selected set of observations and CHIMERE is performed (in moving neighbourhood).

The experimental variogram of the regression residuals is computed and a variogram model is fitted; the model adequacy is checked by cross validation.

Observations are kriged with the CHIMERE model as external drift (in moving neighbourhood). Additional monitoring data, which are not used for calculating the variogram (e.g. data from some mountain sites), are included at this stage.

- For regulatory applications, the choice of the kriging technique and related parameters is adapted to each pollutant, according to cross-validation and validation tests:

For PM_{10}, ordinary co-kriging of the observations (main variable) and CHIMERE (secondary variable) is currently applied. Inclusion of emission density as auxiliary variable and comparison with kriging with external drift are in progress.

For NO_2, kriging with external drift is performed. CHIMERE, NOx emission density and population density are used as external drift.

3. EMEP factsheet

3.1 Assimilation and forecast system: synthesis of the main characteristics

Assimilation and forecast system	
Horizontal resolution	0.125° x 0.0625° lon-lat (native model grid)
Vertical resolution	20 layers (sigma) up to 100 hPa, with approximately 10 in the Planetary Boundary layer
Gas phase chemistry	Evolution of the 'EMEP scheme', comprising 70 species and 140 reactions (Andersson-Sköld and Simpson, 1999; Simpson et al. 2012)
Heterogeneous chemistry	Aerosol-uptake of HNO_3, HO_2 and O_3 (EMEP, 2015)
Aerosol size distribution	2 size fractions $PM_{2.5}$ and $PM_{10\text{-}2.5}$
Inorganic aerosols	MARS (Binkowski and Shankar, 1995), thermodynamic equilibrium for the H^+-NH_4^+-SO_4^{2-}--NO_3^---H_2O system
Secondary organic aerosols	EmChem09soa (Simpson et al., 2012, Bergström et al, 2012)
Aqueous phase chemistry	SO_2 oxidation by ozone and H_2O_2 and metal ion-catalyzed O_2
Dry deposition/sedimentation	Resistance approach for gases and for aerosol, including non-stomatal deposition of NH_3
Mineral dust	Boundary conditions from global C-IFS are used, EMEP dust source inside the model domain
Sea Salt	Boundary conditions from global C-IFS are used
Boundary values	Boundary conditions from global C-IFS are used
Initial values	From end file of D-2 analysis, i.e. valid at D-1, 00UTC
Anthropogenic emissions	CAMS-REG-AP_v3.1/2016
Biogenic emissions	Included
Forecast system	
Meteorological driver	12:00 UTC operational IFS forecast (yesterday's)
Assimilation system	
Assimilation method	Intermittent 3d-var
Observations	NO_2 columns from OMI. NO_2, O_3, SO_2, and PM_{10} surface concentrations, distributed by Meteo-France and INERIS
Frequency of assimilation	Hourly
Meteorological driver	00 UTC operational IFS forecast

3.2 Forward model

The EMEP MSC-W model is a chemical transport model developed at the Norwegian Meteorological Institute under the EMEP programme (UN Convention on Long-range Transboundary Air Pollution). This Eulerian model is developed to be concerned with the regional atmospheric dispersion and deposition of acidifying and eutrophying compounds (S, N), ground level ozone (O_3) and particulate matter ($PM_{2.5}$, PM_{10}). The EMEP MSC-W model system allows several options with regard to the chemical schemes used and the possibility of including aerosol dynamics. Simpson et al. (2012) describes the EMEP MSC-W model in detail, as well as the main model updates since 2006. The forecast version of the EMEP MSC-W model (EMEP-CWF) is in operation since June 2006. The scheduled model updates in CAMS_50 ensure that the model version stays as close as possible to the official EMEP Open Source version. Nevertheless, the EMEP-CWF results and performances in CAMS_50 might differ from those presented in the annual EMEP Status Reports, because of different input data (emissions and meteorological driver) and model run modes (Forecast in EMEP-CWF versus Hindcast in EMEP Status Reports).

3.2.1 Model geometry

The EMEP-CWF covers the European domain [30°N-76°N] x [25°W-45°E] on a geographic projection with a horizontal resolution of 0.125° x 0.0625° (longitude-latitude). Vertically the model uses 20 levels defined as sigma coordinates. The 10 lowest model levels are within the PBL, and the top of the model domain is at 100 hPa.

3.2.2 Forcings and boundary conditions

3.2.2.1 Meteorology

4-day meteorological forecasts from the IFS system of the ECMWF are retrieved daily around 18:15 UTC (12 UTC forecast, used for the EMEP-CWF forecasts) and at 06:15 UTC (00 UTC forecast, used for the EMEP-CWF analyses). The ECMWF forecasts do not include 3D precipitation, which is needed by the EMEP-CWF model. Therefore, a 3D precipitation estimate is derived from large-scale precipitation and convective precipitation (surface variables). Currently the 12 UTC forecast from yesterday's forecast is used, so that there is sufficient time to run the EMEP-CWF well before the deadline for delivery.

3.2.2.2 Chemistry

If available at the start of the forecast run, boundary conditions are taken from the C-IFS. In cases where C-IFS boundary conditions are not available, default boundary conditions are specified for O_3, CO, NO, NO_2, CH_4, HNO_3, PAN, SO_2, isoprene, C_2H_6, some VOCs, Sea salt, Saharan dust and SO_4, as

annual mean concentrations along with a set of parameters for each species describing seasonal, latitudinal and vertical distributions.

Table 3. The chemical and aerosol species taken from C-IFS and used in EMEP. In EMEP 'F' stands for the fine fraction (diameters smaller than 2.5 µm) and 'C' stands for the coarse fraction (diameters between 2.5 and 10 µm). The mapping of IFS size bins into EMEP size bins is based on consideration of typical size distributions. [a]For sea salt a correction factor of 1/4.3 is applied, since C-IFS Sea Salt is calculated for 80% relative humidity while the EMEP Sea Salt contains only the dry component.

C-IFS Species	**Coupled to EMEP Species**	**Comments**
GO_3	O_3	
CO	CO	
NO	NO	
NO_2	NO_2	
PAN	PAN	
HNO_3	HNO_3	
HCHO	HCHO	
SO_2	SO_2	
CH_4	CH_4	
C_5H_8	C_5H_8	
C_2H_6	C_2H_6	
aermr01 (sea salt 0.03-0.5 µm)	SEASALT_F (0-2.5 µm)	SEASALT_F=aermr01/4.3 [a]
aermr02 (sea salt 0.5-5 µm)	SEASALT_C (2.5-10 µm)	SEASALT_C=aermr02/4.3 [a]
aermr03 (sea salt 5-20 µm)		Not used
aermr04 (dust 0.03-0.55 µm)	DUST_SAH_F (0-2.5 µm)	
aermr05 (dust 0.55-0.9 µm)	DUST_SAH_F (0-2.5 µm)	
aermr06 * 0.15 (dust 0.9-20 µm)	DUST_SAH_F (0-2.5 µm)	15% of aermr06 used
aermr06 * 0.35 (dust 0.9-20 µm)	DUST_SAH_C (2.5-10 µm)	35% of aermr06 used
aermr11	SO_4	

3.2.2.3 Surface emissions

CAMS-REG-AP_v3.1/2016 is used, interpolated on the model's native grid, i.e. 0.125° x 0.0625° (lon-lat) resolution.

3.2.3 Dynamical core

The numerical solution of the advection terms of the continuity equation is based on the scheme of (Bott, 1989). The fourth order scheme is utilized in the horizontal directions. In the vertical direction, a second order version applicable to variable grid distances is employed.

3.2.4 Physical parameterisations

3.2.4.1 Turbulence and convection

The turbulent diffusion coefficients (Kz) are first calculated for the whole 3D mode domain on the basis of local Richardson numbers. The planetary boundary layer (PBL) height is then calculated using methods described in (Simpson et al., 2012). For stable conditions, Kz values are retained. For unstable situations, new Kz values are calculated for layers below the mixing height using the O'Brien interpolation (Simpson et al., 2012).

3.2.4.2 Deposition

Parameterisation of dry deposition is based on a resistance formulation, fully described in Simpson et al. (2012). The deposition module makes use of a stomatal conductance algorithm which was originally developed for ozone fluxes, but which is now applied to all gaseous pollutants when stomatal control is important (Emberson et al., 2000; Simpson et al., 2003; Tuovinen et al., 2004). Non-stomatal deposition for NH_3 is parameterised as a function of temperature, humidity, and the molar ratio SO_2/NH_3.

3.2.5 Chemistry and aerosols

The chemical scheme couples the sulphur and nitrogen chemistry to the photochemistry using about 140 reactions between 70 species (Andersson-Sköld and Simpson, 1999; Simpson et al. 2012).

The chemical mechanism is based on the 'EMEP scheme', as well as reactions to cover acidification, eutrophication and ammonium chemistry, as described in Simpson et al., 2012 and references therein.

The standard model version distinguishes 2 size fractions for aerosols, fine aerosol ($PM_{2.5}$) and coarse aerosol ($PM_{2.5-10}$). The aerosol components presently accounted for are SO_4, NO_3, NH_4, anthropogenic primary PM and sea salt. Also aerosol water is calculated. Dry deposition parameterisation for aerosols follows standard resistance-formulations, accounting for diffusion, impaction, interception, and sedimentation. Wet scavenging is treated with simple scavenging ratios, taking into account in-cloud and sub-cloud processes. For secondary organic aerosol (SOA) the so-called EmChem09soa scheme is used, which is a somewhat simplified version of the mechanisms discussed in detail by Bergström et al. (2012).

3.3 Assimilation system

The EMEP data assimilation system (EMEP-DAS) is based on the 3D-Var implementation for the MATCH model (Kahnert, 2009). The background error covariance matrix is estimated following the NMC method (Parrish and Derber, 1992). The EMEP-DAS is described in detail in Valdebenito B. and Heiberg (2009), Valdebenito B. et al. (2010) and Valdebenito B. and Tsyro (2012).

The EMEP-DAS delivers analyses of yesterday (driven by the operational IFS forecast of 00UTC of yesterday) for NO_2, using NO_2 columns of OMI and in-situ measurements of NO_2 surface concentrations. For ozone, SO_2, and PM_{10}, only surface measurements are assimilated. CO surface observations can be assimilated, but this feature is currently switched off in the operational chain as it does not lead to a significant improvement. EMEP-DAS has been in operation since November 2012, with the following major updates (see also 'Evolutions in the EMEP suite'):

- October 2012: version rv4.1, including DA of NO_2.
- June 2013: version rv4.4.
- May 2014: version rv4.5.
- January 2015: ozone DA included.
- December 2016: version rv4.10 (this corresponds to the EMEP Open Source version publicly available at https://github.com/metno/emep-ctm/releases/tag/rv4_10, with only some minor modifications in the pollen and DA modules).
- December 2016: SO_2 DA included.
- November 2017: update to version rv4.15. This version corresponds to the EMEP Open Source that was publicly available at https://github.com/metno/emep-ctm at the time, except for the chemistry module (EmChem09 is used in CAMS_50, while EmChem16 is used in the Open Source version) as well as some minor modifications in the pollen and DA modules.
- September 2018: update to version rv4.17a (but still with chemistry module EmChem09).
- September 2018: PM_{10} DA included.
- June 2019: update to version rv4.33 (but still with chemistry module EmChem09).

4. EURAD-IM factsheet

4.1 Assimilation and forecast system: synthesis of the main characteristics

Assimilation and forecast system	
Horizontal resolution	9 km on a Lambert conformal projection
Vertical resolution	23 layers up to 100 hPa Lowest layer thickness about 35 m About 15 layers below 2 km
Gas phase chemistry	RACM-MIM
Heterogeneous chemistry	N_2O_5 hydrolysis: RH dependent parameterisation
Aerosol size distribution	3 log-normal modes: 2 fine + 1 coarse, fixed standard deviation
Inorganic aerosols	Thermodynamic equilibrium for the H^+-NH_4^+-SO_4^{2-}--NO_3^---H_2O system
Secondary organic aerosols	Updated SORGAM module
Aqueous phase chemistry	10 gas/aqueous phase equilibria 5 irreversible S(IV) -> S(VI) transformations
Dry deposition/sedimentation	Resistance approach/size dependent sedimentation velocity
Mineral dust	DREAM model
Sea Salt	Included
Boundary values	C-IFS forecast
Initial values	3d-var analysis for the previous day
Anthropogenic emissions	CAMS-REG-AP_v3.1/2016
Biogenic emissions	MEGAN V2.10 (Guenther et. al, 2012) Hourly GFAS wild fire emission data
Forecast system	
Meteorological driver	WRF forced by 12:00 UTC operational IFS forecast for the previous day
Assimilation system	
Assimilation method	Intermittent 3d-var
Observations	NRT surface in-situ data distributed by Meteo-France and INERIS, NO_2 and SO_2 column retrievals from Aura/OMI and MetOp/GOME-2, MOPITT CO profiles, IASI CO partial columns
Frequency of assimilation	Hourly
Meteorological driver	WRF forced by the operational IFS analysis for the previous day

4.2 Forward model

The EURAD-IM system consists of 5 major parts: the meteorological driver WRF, the pre-processors EEP and PREP for preparation of anthropogenic emission data and observations, the EURAD-IM Emission Model EEM, and the chemistry transport model EURAD-IM (Hass et al., 1995, Memmesheimer et al., 2004). EURAD-IM is a Eulerian meso-scale chemistry transport model involving advection, diffusion, chemical transformation, wet and dry deposition and sedimentation of tropospheric trace gases and aerosols. It includes 3d-var and 4d-var chemical data assimilation (Elbern et al., 2007) and is able to run in nesting mode.

4.2.1 Model geometry

To cover the CAMS domain from 25°E to 45°W and 30°N to 72°N, 2 Lambert conformal projections with 45 km (199x166 grid boxes) and 9 km horizontal resolution (581x481 grid boxes) are used (see Figure 2). The model domain with the finer resolution covering the entire European part of the CAMS domain is nested within the halo domain with the coarser resolution.

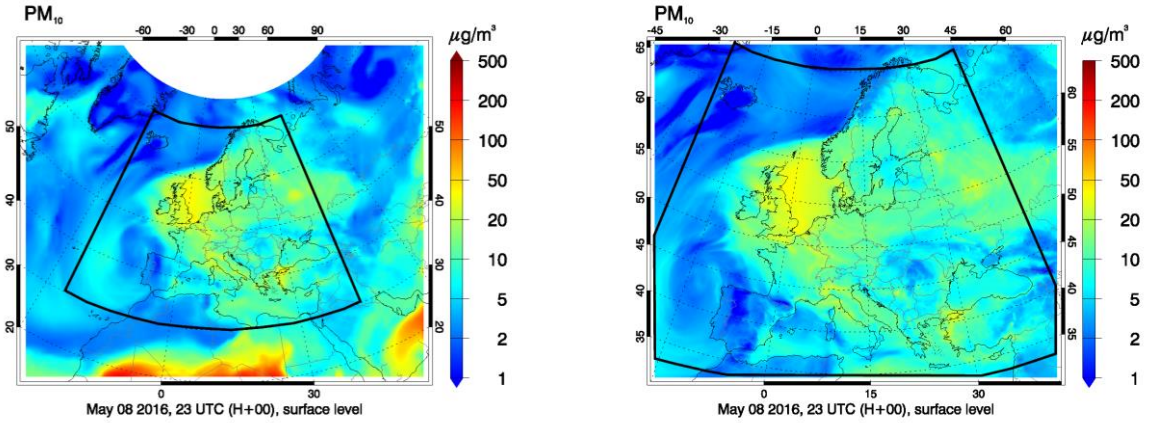

Figure 2 - EURAD-IM halo grid (left) and EURAD-IM nest with 15km horizontal resolution (right) used to cover the CAMS model domain (black line)

Variables are horizontally staggered using an Arakawa C grid. Vertically, the atmosphere is divided by 23 terrain-following sigma coordinate layers between the surface and the 100 hPa pressure level. About 15 layers are below 2 km height. The thickness of the lowest layer is about 35 m. Both the EURAD-IM CTM and the WRF model use the same Lambert conformal projection and horizontal and vertical staggering of variables.

4.2.2 Forcings and boundary conditions

4.2.2.1 Meteorology

The Weather Research and Forecast (WRF) model is used for the calculation of meteorological fields needed to drive the EURAD-IM CTM. Initial and boundary values for the WRF simulations are derived from IFS meteorological fields. Nudging of IFS data is not applied. The IFS operational 12:00 UTC forecast for the previous day is used for the provision of initial and boundary values for the WRF forecast. IFS data on 18 pressure levels between the surface and 30 hPa with a temporal resolution of 3 hours is horizontally and vertically interpolated by the WRF Pre-processing System (WPS). For the EURAD-IM air quality analysis, WRF simulations based on the operational IFS analysis for the times 00:00, 06:00, 12:00, and 18:00 UTC are used. For both the EURAD-IM forecast and analysis, hourly WRF output is temporally linearly interpolated within the EURAD-IM CTM to calculate meteorological variables at the transport time steps. EURAD-IM and WRF are using the same horizontal staggering of meteorological variables (Arakawa-C grid) on the same Lambert conformal projection. In addition both models use the same terrain following sigma coordinate. This enables a direct use of meteorological variables for the air quality simulation without additional horizontal and vertical interpolation steps. Mainly for this reason a calculation of meteorological fields with WRF is preferred to a direct use of IFS data.

4.2.2.2 Chemistry

For the provision of chemical gas phase and aerosol phase boundary values for the operational EURAD-IM air quality forecast and analysis, the C-IFS 00:00 UTC forecast for the previous day is directly extracted from the MARS archive at ECMWF (class=mc, expver=0001, type=fc). C-IFS data at 36 model levels with a temporal resolution of 3 hours is horizontally and vertically interpolated on the lateral boundaries of the halo domain with 45 km horizontal resolution used by the EURAD-IM CTM (see Table 4).

Use of Sea Salt from C-FIS using a scaling factor of 4.3 is under investigation.

Table 4. The chemical and aerosol species taken from C-IFS and used in EURAD-IM

C-IFS Species	**Coupled to EURAD-IM Species**	**Comments**
CO	CO	
C_2H_6	ETH	ethane
HCHO	HCHO	
HNO_3	HNO_3	
C_5H_8	ISO	isoprene
NO	NO	
NO_2	NO_2	

C-IFS Species	Coupled to EURAD-IM Species	Comments
GO_3	O_3	
PAN	PAN	
SO_2	SO_2	
Mineral dust	Mineral dust	95% coarse mode mineral dust, 5% accumulation mode mineral dust
Organic matter hydrophobic	Organic carbon	80% accumulation, 20% Aitken mode
Organic matter hydrophilic	Organic carbon	80% accumulation mode, 20% Aitken mode
Black carbon hydrophobic	Elemental carbon	70% accumulation mode, 30% Aitken mode
Black carbon hydrophilic	Elemental carbon	70% accumulation mode, 30% Aitken mode
Sulfate	SO_4	90% accumulation mode, 10% Aitken mode
Sea salt		Currently not used because of wet / dry mass discrepancy

4.2.2.3 Surface emissions

CAMS-REG-AP_v3.1/2016 is used for anthropogenic emissions. Yearly total emission amounts are area weighted horizontally interpolated on the EURAD-IM model grid. The VOC and PM split, the vertical distribution of area sources and the emission strength per hour is calculated within the EURAD-IM CTM based on profiles from the CAMS-REG-AP_v3.1/2016 inventory. For the vertical distribution of point sources profiles are taken partly from the EURAD-IM Emission Model (EEM) and partly from the CAMS-REG-AP_v3.1/2016 inventory. The VOC and PM split depends on source category and country, the vertical distribution only on source category. For the temporal distribution of emissions monthly, weekly and daily profiles depending on source category are used. Temporal profiles are shifted according to local time.
Biogenic emissions are calculated in the EURAD-IM CTM with the Model of Emissions of Gases and Aerosols from Nature (MEGAN) (Guenther et al., 2012). Emissions from fires are taken into account, using the Global Fire Assimilation System Version 1.2 (GFASv1.2) product (Kaiser et al., 2012) available daily with hourly temporal resolution at 0.1° x 0.1° horizontal resolution. Zero fire emissions are used for D+2 and D+3 forecasts. Emissions of birch, olive, grass and ragweed pollen are calculated within the EURAD-IM CTM dependent on meteorological conditions, according to algorithms provided by the FMI (Sofiev et al., 2015; Sofiev et al., 2017).

4.2.3 Dynamical core

To propagate a set of chemical constituents forward in time, the EURAD-IM CTM solves a system of partial differential equations:

$$\frac{\partial c_i}{\partial t} = -\nabla(\vec{\boldsymbol{v}}\, c_i) + \nabla(\rho \mathbf{K} \nabla \frac{c_i}{\rho}) + A_i + E_i - S_i\,,$$

where c_i is the mean mass mixing ratio of chemical species i, ***v*** are mean wind velocities, **K** is the eddy diffusivity tensor, ρ is air density, A_i is the chemical generation term for species i, E_i and S_i its emission and removal fluxes, respectively. The numerical solution of the above equation has its difficulties, due to the different numerical characters of the major processes. To overcome these problems an operator splitting technique is employed (McRae, 1982), wherein each process is independently treated in a sequence. The EURAD-IM CTM uses a symmetric splitting of the dynamical processes, encompassing the chemistry solver **C**:

$$c_i^{t+\Delta t} = T_h\, T_v\, D_v\, C\, D_v\, T_v\, T_h\, c_i^t,$$

where $T_{h,v}$ and D_v denote transport and diffusion operators in horizontal (h) and vertical (v) direction. The emission term is included in **C**.
The CTM's basic time-step Δt depends on the horizontal and vertical grid resolution in order to fulfil the CFL-criterion. If this criterion is locally not fulfilled, the time-step is dynamically adapted. $\Delta t_T = \Delta t/2$ is the transport time step used for the advection and diffusion with operators $T_{h,v}$ and D_v. For the gas phase chemistry calculations, the basic time step Δt is split into a set of variable time steps, which are often considerably smaller than Δt according to the chemical situation.

The positive definite advection scheme of Bott (1989), implemented in a one-dimensional realisation, is used to solve the advective transport.

4.2.4 Physical parameterisations

4.2.4.1 Turbulence and convection

An Eddy diffusion approach is used to parameterize the vertical sub-grid-scale turbulent transport. The calculation of vertical Eddy diffusion coefficients is based on the specific turbulent structure in the individual regimes of the planetary boundary layer (PBL) according to the PBL height and the Monin-Obukhov length (Holtslag and Nieuwstadt, 1986). A semi-implicit (Crank-Nicholson) scheme is used to solve the diffusion equation.

The sub-grid cloud scheme in EURAD-IM was derived from the cloud model in the EPA Models-3 Community Multiscale Air Quality (CMAQ) modelling system (Roselle and Binkowski, 1999). Convective cloud effects on both gas phase species and aerosols are considered.

4.2.4.2 Deposition

The gas phase dry deposition modelling follows the method proposed by Zhang et al. (2003). Dry deposition of aerosol species is treated size dependent, using the resistance model of Petroff and Zhang (2010) with consideration of the canopy. Dry deposition is applied as lower boundary condition of the diffusion equation.

Wet deposition of gases and aerosols is derived from the cloud model in the CMAQ modelling system (Roselle and Binkowski, 1999). The wet deposition of pollen is treated according to Baklanov and Sorenson, 2001.
Size dependent sedimentation velocities are calculated for aerosol and pollen species. The sedimentation process is parameterized with the vertical advective transport equation and solved using the fourth order positive definite advection scheme of Bott (1989).

4.2.5 Chemistry and aerosols

In the EURAD-IM CTM, the gas phase chemistry is represented by an extension of the Regional Atmospheric Chemistry Mechanism (RACM) (Stockwell et al., 1997) based on the Mainz Isoprene Mechanism (MIM) (Geiger et al., 2003). A 2-step Rosenbrock method is used to solve the set of stiff ordinary differentials equations (Sandu and Sander, 2006). Photolysis frequencies are derived using the FTUV model according to Tie et al. (2003). The radiative transfer model therein is based on the Tropospheric Ultraviolet-Visible Model (TUV) developed by Madronich and Weller (1990).

The modal aerosol dynamics model MADE (Ackermann et al., 1998) is used to provide information on the aerosol size distribution and chemical composition. To solve for the concentrations of the secondary inorganic aerosol components, a FEOM (fully equivalent operational model) version, using the HDMR (high dimensional model representation) technique (Rabitz et al., 1999, Nieradzik, 2005), of an accurate mole fraction based thermodynamic model (Friese and Ebel, 2010) is used. The updated SORGAM module (Li et al., 2013) simulates secondary organic aerosol formation.

4.3 Assimilation system

The EURAD-IM assimilation system includes (i) the EURAD-IM CTM and its adjoint, (ii) the formulation of both background error covariance matrices for the initial states and the emission, and their treatment to precondition the minimisation problem, (iii) the observational basis and its related error covariance matrix, and (iv) the minimisation including the transformation for preconditioning. The

quasi-Newton limited memory L-BFGS algorithm described in Nocedal (1980) and Liu and Nocedal (1989) is applied for the minimisation.

The 3-dimensional variational data assimilation version of the EURAD-IM aims to minimise the following cost function:

$$J(\boldsymbol{x}) = \frac{1}{2}\left[\boldsymbol{x}-\boldsymbol{x}^{\mathrm{b}}\right]^{T}\mathbf{B}^{-1}\left[\boldsymbol{x}-\boldsymbol{x}^{\mathrm{b}}\right] + \frac{1}{2}\left[\boldsymbol{y}-H(\boldsymbol{x})\right]^{T}\mathbf{R}^{-1}\left[\boldsymbol{y}-H(\boldsymbol{x})\right]$$

with **x** being the current model state with background knowledge $\mathbf{x}^{b}$, H the observation operator, **B** the background error covariance matrix, **R** the observation error covariance matrix and **y** a set of observations. The minimum will be found by evaluating the gradient of the cost function with respect to the control variables **x**,

$$\nabla_{\boldsymbol{x}} J = \mathbf{B}^{-1}\left[\boldsymbol{x}-\boldsymbol{x}^{\mathrm{b}}\right] + \mathbf{H}^{T}\mathbf{R}^{-1}\left[\boldsymbol{y}-H(\boldsymbol{x})\right]$$

with $\mathbf{H}^{T}$ being the adjoint of the observation operator H. The observation operator is needed to get the model equivalent to each type of measurement, yielding the possibility to compare the model state to various kinds of observations. A powerful observation operator is implemented in the current version of the EURAD-IM data assimilation system, to assimilate heterogeneous sources of information like ground-based in-situ measurements as well as retrieval products of satellite observations, even using averaging kernel information.
Following Weaver and Courtier (2001) with the promise of a high flexibility in designing anisotropic and heterogeneous influence radii, a diffusion approach for providing **B** is implemented. Weaver and Courtier show that the diffusion equation serves as a valid operator for square-root covariance operator modelling by suitable adjustments of local diffusion coefficients. For a detailed description of the properties of the implemented background error covariance modelling, as well as the observation error covariance matrix **R**, see Elbern et al. (2007).

Currently assimilated in the EURAD-IM analysis and interim re-analysis are NRT surface in-situ observations of O_3, NO, NO_2, SO_2, $PM_{2.5}$, PM_{10} and remote sensing data from several instruments: NO_2 and SO_2 column retrievals from Aura/OMI and MetOp/GOME-2, MOPITT CO profiles, and IASI CO partial columns. Aircraft in-situ data for O_3, CO and NO_x from IAGOS are additionally assimilated in the validated re-analysis.

5. LOTOS-EUROS factsheet

5.1 Assimilation and forecast system: synthesis of the main characteristics

Assimilation and forecast system	
Horizontal resolution	0.1° (longitude) x 0.1° (latitude)
Vertical resolution	5 layers, top at 5 km above sea level
Gas phase chemistry	Modified version of the original CBM-IV
Heterogeneous chemistry	N_2O_5 hydrolysis
Aerosol size distribution	Bulk approach: $PM_{2.5}$ and $PM_{2.5-10}$
Inorganic aerosols	ISORROPIA-2
Secondary organic aerosols	Not included in this version
Aqueous phase chemistry	Linearized
Dry deposition/sedimentation	Resistance approach, following Erisman et al. (1994). Zhang (2001) deposition scheme is used for particles, explicitly including particle size and sedimentation
Mineral dust	Emissions after Marticorena &Bergametti (1995) with soil moisture inhibition as described by Fécan et al (1999)
Sea Salt	Parameterised based on wind speed at 10m following (Monahan et al., 1986) and sea-surface temperature (Martensson et al., 2003)
Boundary values	CAMS-global forecast (lateral and top)
Initial values	24h forecast from the day before
Anthropogenic emissions	CAMS-REG inventory
Biogenic emissions	Following Guenther et al. (1993) using 115 tree types over Europe
Forecast system	
Meteorological driver	12:00 UTC operational IFS forecast for the day before
Assimilation system	
Assimilation method	Ensemble Kalman filter
Observations	In-situ surface observations (O_3, NO_2, PM_{10}, $PM_{2.5}$) distributed by Meteo-France as well as OMI NO_2
Frequency of assimilation	Hourly, performed once a day for the previous day
Meteorological driver	00:00 UTC operational IFS forecast for the same day

5.2 Forward model

The LOTOS-EUROS model is a 3D chemistry transport model aimed to simulate air pollution in the lower troposphere. The model has been used in a large number of studies for the assessment of particulate air pollution and trace gases (e.g. O_3, NO_2) (e.g. Manders et al. 2009, Hendriks et al, 2013, Curier et al, 2012, 2014, Schaap et al 2013). The model has participated frequently in international model comparisons addressing ozone (e.g. Solazzo et al. 2012a) and particulate matter (e.g. Solazzo et al. 2012b, Stern et al. 2008). For a detailed description of the model as well as for references not found in the references section of this document, we refer to Manders et al. (2017).

5.2.1 Model geometry

The domain of LOTOS-EUROS is the CAMS regional domain from 25°W to 45°E and 30°N to 70°N. The projection is regular longitude-latitude, at 0.1°x0.1° grid spacing. In the vertical, there are currently 4 dynamic layers and a surface layer. The standard model version extends in vertical direction 5 km above sea level. The lowest dynamic layer is the mixing layer, followed by 3 reservoir layers. The heights of the reservoir layers are determined by the difference between the mixing layer height and 5 km. Simulations incorporate a surface layer of a fixed depth of 25 m. For output purposes, the concentrations at measuring height (usually 2.5 m) are diagnosed by assuming that the flux is constant with height and equal to the deposition velocity times the concentration at height *z*.

5.2.2 Forcings and boundary conditions

5.2.2.1 Meteorology

The LOTOS-EUROS system in its standard version is driven by 3-hourly meteorological data. These include 3D fields for wind direction, wind speed, temperature, humidity and density, substantiated by 2D gridded fields of mixing layer height, precipitation rates, cloud cover and several boundary layer and surface variables. In CAMS, meteorological forecast data obtained from the ECMWF is used to force the model.

5.2.2.2 Chemistry

The lateral and top boundary conditions for trace gases and aerosols are obtained from the CAMS-global daily forecasts (see Table 5). As mentioned in paragraph 5.1, LOTOS-EUROS uses a bulk approach for the aerosol size distribution differentiating between a fine and a course fraction but for dust and sea salt there are distinct, more detailed size classes, more specifically dust_ff, dust_f, dust_c, dust_cc, dust ccc, na_f, na_c, na_cc and na_ccc. The assumption as regards the diameters for those species are:_ff: 0.1-1 µm, _f:1-2.5 µm, ccc: 2.5-4 µm, _cc: 4-7 µm, _c:7-10 µm.

Table 5. The chemical and aerosol species taken from C-IFS and used in LOTOS-EUROS

CAMS-global Species	**Coupled to LOTOS-EUROS Species**	**Comments**
GO_3	O_3	
CO	CO	
NO	NO	
NO_2	NO_2	
PAN	PAN	
HNO_3	HNO_3	
HCHO	form	
SO_2	SO_2	
CH_4	CH_4	
C_5H_8	isop	
aermr01 (0.06-1 µm)	na_ff	Divided by 4.3 to reduce to dry sea salt
aermr02 (1-10 µm)	na_f, na_ccc, na_cc, na_c	Divided by 4.3 to reduce to dry sea salt. Distributed as follows: 10% to na_f, 20% to na_ccc, 40% to na_cc and 30% to na_c
aermr04 (0.06-1.1 µm)	dust_ff, dust_f, dust_ccc, dust_cc, dust_c	Distributed as follows: 2% to dust_ff, 8% to dust_f, 10% to dust_ccc, 40% to dust_cc and 40% to dust_c
aermr05 (1.1-1.8 µm)	dust_ff, dust_f, dust_ccc, dust_cc, dust_c	Distributed as follows: 2% to dust_ff, 8% to dust_f, 10% to dust_ccc, 40% to dust_cc and 40% to dust_c
aermr06 (1.8-40 µm)	dust_ff, dust_f, dust_ccc, dust_cc, dust_c	Distributed as follows: 2% to dust_ff, 8% to dust_f, 10% to dust_ccc, 40% to dust_cc and 40% to dust_c
aermr07	ec_f	
aermr08	ec_f	
aermr09	pom_f	
aermr10	pom_f	
aerm11	so4a_f	

For dust species, all C-IFS compounds (aerm04, aerm05 and aerm06) are summed up before being distributed in the LOTOS-EUROS bins indicated on the right.

When the dynamic boundaries from C-IFS are missing, the model uses climatological boundary concentrations derived from C-IFS data.

5.2.2.3 Land use

The land use is taken from the CORINE/Smiatek database enhanced with the 3 species map for Europe made by (Koeble and Seufert, 2001). The combined database has a resolution of 0.0166x0.0166°, which is aggregated, to the required resolution during the start-up of a model simulation.

5.2.2.4 Surface emissions

The anthropogenic emissions currently used are those of CAMS-REG-AP_v3.1/2016, which cover years 2000-2011 (Kuenen et al., 2014). From v1.8, the use of the stack height distribution from the EuroDelta study is implemented, which is per SNAP (or more recently, GNFR) category. Time profiles used are defined per country and GNFR emission category type (SNAP or GFNR). Biogenic isoprene emissions are calculated following the mathematical description of the temperature and light dependence of the isoprene emissions, proposed by (Guenther et al., 1993), using actual meteorological data. Sea salt emissions are parameterised following (Monahan et al., 1986) from the wind speed at 10-meter height. The fire emissions are taken from the near real-time GFAS fire emissions database.

Mineral dust emissions are calculated online based on the sand blasting approach by Marticorena & Bergametti (1995) with soil moisture inhibition as described by Fécan et al (1999). For wind speed, a roughness length of 0.013 m was used for bare soil, for the parameterisation of dust emissions a local (effective) roughness length of $8x10^{-4}$ m was used, with a smooth roughness length of $3x10^{-5}$ m. For the threshold friction velocity a tuning factor of 0.66 was used (Heinold et al (2007). The sandblasting efficiency was calculated according to Shao et al (1996). Soil characteristics were derived from the STATSGO maps based on the work by Zobler (1986) with USGS soil texture classes. A simple preferential sources map, based on topographical differences in a radius of 10 degrees, was derived following the approach by Ginoux et al (2001). In addition, a tuning constant of 0.5 was used to modify the total emission strength.

5.2.3 Dynamical core

The transport consists of advection in 3 dimensions, horizontal and vertical diffusion, and entrainment/detrainment. The advection is driven by meteorological fields (u,v), which are input every 3 hours. The vertical wind speed w is calculated by the model as a result of the divergence of the horizontal wind fields. The improved and highly accurate, monotonic advection scheme developed by (Walcek, 2000) is used to solve the system. The number of steps within the advection scheme is chosen such that the Courant restriction is fulfilled.

5.2.4 Physical parameterisations

5.2.4.1 Turbulence and convection

Entrainment is caused by the growth of the mixing layer during the day. Each hour the vertical structure of the model is adjusted to the new mixing layer depth. After the new structure is set, the pollutant concentrations are redistributed using linear interpolation. Vertical diffusion is described using the standard K_z theory. Vertical exchange is calculated employing the new integral scheme by (Yamartino et al., 2004).

Atmospheric stability values and functions, including Kz values, are derived using standard similarity theory profiles.

5.2.4.2 Deposition

The dry deposition in LOTOS-EUROS is parameterised following the well-known resistance approach. The laminar layer resistance and the surface resistances for acidifying components and particles are described following the EDACS system (Erisman et al., 1994). Wet deposition is divided between in-cloud and below-cloud scavenging. The in-cloud scavenging module is based on the approach described in Seinfeld and Pandis (2006) and Banzhaf et al. (2012).

5.2.5 Chemistry and aerosols

LOTOS-EUROS uses the TNO CBM-IV scheme, which is a modified version of the original CBM-IV (Whitten et al., 1980). N_2O_5 hydrolysis is described explicitly based on the available (wet) aerosol surface area (using $\gamma = 0.05$) (Schaap et al., 2004). Aqueous phase and heterogeneous formation of sulphate is described by a simple first order reaction constant (Schaap et al., 2004; Barbu et al., 2009). Aerosol chemistry is represented using ISORROPIA II (Fountoukis, 2007).

5.3 Assimilation system

The LOTOS-EUROS model is equipped with a data assimilation package with the ensemble Kalman filter technique (Curier et al., 2012). The ensemble is created by specification of uncertainties for emissions (NOx, VOC, NH_3 and aerosol), ozone deposition velocity, and ozone top boundary conditions. Currently, data assimilation is performed for O_3, NO_2, PM_{10} and $PM_{2.5}$, using surface observations collected and provided by Meteo-France each morning for the day before. OMI NO_2 is also assimilated.

6. MATCH factsheet

6.1 Assimilation and forecast system: synthesis of the main characteristics

Assimilation and forecast system	
Horizontal resolution	0.1° regular lat-lon grid
Vertical resolution	26 levels (using reduction of IFS levels), 10 layers in the boundary layer (below 850 hPa)
Gas phase chemistry	Based on EMEP (Simpson et al., 2012), with modified isoprene chemistry (Carter, 1996; Langner et al., 1998)
Heterogeneous chemistry	HNO_3-formation from N_2O_5; equilibrium reactions for NH_3-HNO_3
Aerosol size distribution	2bins: 0.01–2.5, 2.5–10 µm
Inorganic aerosols	Sulphate, Nitrate, Ammonium
Secondary organic aerosols	Based on Bergström, 2015, Bergström et al., 2018, Hodzic 2016, Lane et al., 2014, and Ots et al., 2016
Aqueous phase chemistry	SO_2 oxidation by H_2O_2 and O_3
Dry deposition/sedimentation	Deposition scheme from the EMEP MSC-W model, Simpson et al., Atmos Chem Phys 12, 7825-7865 (2012)
Mineral dust	Road dust emissions are based on the formulation by Schaap et al. (2009). A factor 2.5 higher emissions is assumed related to studded tyres in the period Feb-April based on Omstedt et al. (2005).
Sea Salt	Based on parameterisation by Sofiev et al. (2011)
Boundary values	C-IFS forecast for the day before (zero boundaries for sea-salt)
Initial values	MATCH 24h forecasts from the day before
Anthropogenic emissions	CAMS-REG-AP_v3.1/2016
Biogenic emissions	Isoprene (Simpson, 1995; updated biogenic emissions of isoprene and monoterpenes, based on Simpson et al., 2012, implemented but not yet in operational version)
Forecast system	
Meteorological driver	12:00 UTC operational IFS forecast for the day before (0.1°, 78 levels)
Assimilation system	
Assimilation method	Intermittent 3Dvar data assimilation embedded in the MATCH model

Observations	NRT in-situ observations (O_3, NO_2, CO, SO_2, PM_{10}, $PM_{2.5}$) distributed by Meteo-France
Frequency of assimilation	Hourly, performed once a day for the previous day
Meteorological driver	IFS forecast and analyses 00Z for the same day (0.2°, 26 levels, reduction of IFS levels)

6.2 Forward model

The Multi-scale Atmospheric Transport and Chemistry model (MATCH) is an off-line chemical transport model (CTM) with a flexible design, accommodating different weather data forcing on different resolutions and projections, and a range of alternative schemes for deposition and chemistry.

In CAMS, MATCH is forced by IFS weather data from ECMWF MARS archive.

6.2.1 Model geometry

The model geometry is taken from the input weather data. The vertical resolution is reduced with respect to the ECMWF operational model by combining pairs of IFS layers; hybrid vertical coordinates are used. The horizontal geometry is defined when retrieving the weather data from the MARS system (currently a lat-long grid with 0.2° resolution). The lowest 52 layers of the ECMWF model are used for the air quality simulations. The model top is at ca 8000 m height. The model domain covers the area between 28.8° W to 45.8° E and 29.2° N to 70.0° N. The grid is an Arakawa C-grid with staggered wind components.

6.2.2 Forcings and boundary conditions

6.2.2.1 Meteorology

2 sets of IFS data are used during a diurnal cycle retrieved on 0.1° resolution for the forecast model and 0.2° resolution for the analyses. The model forecast using IFS starting at 12Z the day before the first forecast day, while the data assimilation is based on the 00Z analysis from the same day as valid for the MATCH analyses.

6.2.2.2 Chemistry

The operational MATCH CAMS version uses dynamical boundary concentrations from the global CAMS C-IFS model for the following species: O_3, CO, HCHO, NO, NO_2, SO_2, HNO_3, PAN, CH_4, C_5H_8, o-xylene, sulphate and C_2H_6 (see Table 6); these boundaries are updated every 3 hours. The model top boundary is defined as the mean of the horizontal boundaries at the model top (due to empty global

boundaries in the internal of the domain). The dynamic boundary fields are re-distributed in the vertical in a mass-conservative way, to fit into the vertical hybrid coordinates used by ECMWF.

Table 6. The chemical and aerosol species taken from C-IFS and used in MATCH

C-IFS Species	**Coupled to MATCH Species**	**Comments**
HCHO	HCHO	
CO	CO	
C_2H_6	C_2H_6	
SULFATE	SULFATE	
NO_2	NO_2	
NO	NO	
HNO_3	HNO_3	
PAN	PAN	
SO_2	SO_2	
CH_4	CH_4	
GO_3	O_3	
aermr07	EC_2_5	IFS size bins merged a)
aermr07	EC_coarse	IFS size bins merged a)
aermr09	OC_2_5	IFS size bins merged a)
aermr09	OC_coarse	IFS size bins merged a)
aermr04, aermr05,aermr06	DUST_2_5	IFS size bins merged b)
aermr04, aermr05,aermr06	DUST_coarse	IFS size bins merged b)
aermr01, aermr02	NACL_2_5	IFS size bins merged c)
aermr01, aermr02	NACL_coarse	IFS size bins merged c)
aerm11	SULFATE	Upcoming in CIFS-137
Aerm16	NO_4NO_3	Upcoming in CIFS-137
Aerm17	NITRATE	Upcoming in CIFS-137
Aerm18	NH_42SO_4	Upcoming in CIFS-137

The conversion from C-IFS bins and fine and coarse mode follows advice from Miha Razinger (ECMWF).

a) Conversion between IFS EC/OC and MATCH two bins for EC/OC
EC_2_5 =0.7* aermr07
EC_coarse=0.15*aermr07

OC_2_5 =0.7* aermr09
OC_coarse=0.15*aermr09

b) Conversion between IFS DUST and MATCH two bins for DUST
DUST_2_5 = 1* aermr04 + 1* aermr05 + 0.11* aermr06

DUST_coarse=0.44*aermr06

c) Conversion between IFS NACL and MATCH two bins for NACL
NACL_2_5 = 1* aermr01/4.3 + 0.4* aermr02/4.3
NACL_coarse = 0.6*aermr02/4.3

For the other model species fixed boundary conditions are used, in most cases with seasonal variation.

When the dynamic boundaries from C-IFS are missing, the model uses climatological boundary concentrations instead – this means the model will run with reasonable boundaries even when the global data are missing.

6.2.2.3 Land use

The current operational system using various tiles of physiography derived from CCS/SEI inventory.

6.2.2.4 Anthropogenic emissions

The present CAMS version of MATCH uses CAMS-REG-AP_v3.1/2016 (split into 10 GNFR classes).

6.2.3 Dynamical core

Mass conservative transport schemes are used for advection and turbulent transport. The advection is formulated as a Bott-like scheme (see Robertson et al., 1999). A second order transport scheme is used in the horizontal as well as the vertical. The vertical diffusion is described by an implicit mass conservative first order scheme, where the exchange coefficients for neutral and stable conditions are parameterized following Holtslag et al. (1991). In the convective case the turbulent Courant number is directly determined from the turnover time in the ABL.

Part of the dynamical core is the initialisation and adjustment of the horizontal wind components. This is a very important step to ensure mass conservative transport. The initialisation is based on a procedure proposed by Heimann and Keeling (1989), where the horizontal winds are adjusted by means of the difference between the input surface pressure tendency, and the calculated pressure tendency assumed to be an error in the divergent part of the wind field.

6.2.4 Physical parameterisations

6.2.4.1 Turbulence and convection

Boundary layer parameterisation is based on surface heat and water vapour fluxes as described by van Ulden and Holtslag (1985) for land surfaces, and Burridge and Gadd (1977) for sea surfaces. The boundary layer height is calculated from formulations proposed by Zilitinkevich and Mironov (1996) for the neutral and stable case, and from Holtslag et al. (1995) for the convective case. These parameterisations drive the formulations for dry deposition and vertical diffusion.

6.2.4.2 Deposition

Dry deposition of gases and aerosols is modelled using a simple resistance approach, which depends on surface type and season[3]; the deposition of gases to vegetated surfaces is coupled to soil moisture, temperature, vapour pressure deficit, and photo synthetically active radiation. The wet scavenging is assumed to be proportional to the precipitation intensity for most gaseous and aerosol components.

6.2.5 Chemistry and aerosols

The photochemistry scheme is based on the standard EMEP MSC-W chemistry scheme (Simpson et al., 2012), with a modified scheme for isoprene, based on the so-called Carter-1 mechanism (Carter, 1996; Langner et al., 1998). The SOA description is based on Hodzic et al., 2016 (Atmos. Chem. Phys. 2016, 16, 7917).

6.3 Assimilation system

The model for data assimilation is an integrated part of the MATCH modelling system. The data assimilation scheme as such is a variational spectral scheme (Kahnert, 2008), implying that the background covariance matrices are modelled in spectral space. The limitation is that covariance structures are described as isotropic and homogeneous. The advantage is that the background error matrix becomes block diagonal, and there are no scale separations as the covariance between spectral components are explicitly handled. The block diagonal elements are the covariance between wave components at model layers and chemical compounds.

Modelling the background error covariance matrices is the central part in data assimilation. This is conducted by means of the so-called NMC approach (Parish and Derber, 1992). The CTM (MATCH) is run for a 3-month period for photochemistry and aerosols with analysed and forecasted ECMWF

[3] For a few components, the deposition is also affected by snow cover: O_3, NO_2, SO_2, H_2O_2; or sub-zero temperatures: O_3.

weather data. The differences are assumed to mimic the background errors, and the statistics in spectral space are generated for different combinations of the model compounds:

- O_3, NO_2, NO
- SO_2
- CO
- $PM_{2.5}$, PM_{10}

The scheme is fully intermittent in hour-by-hour steps and the above-listed components are assimilated from in-situ measurements. The following unobserved components are indirectly assimilated through the projection of the forecast model: NMVOCs, PAN and NH_3.

7. MOCAGE factsheet

7.1 Assimilation and forecast system: synthesis of the main characteristics

Assimilation and forecast system	
Horizontal resolution	0.1° regular lat-lon grid for forecast 0.2° regular lat-lon grid for assimilation
Vertical resolution	47 layers up to 5 hPa Lowest layer thickness about 40 m About 8 layers below 2 km
Gas phase chemistry	RACM (tropospheric) and REPROBUS (stratospheric)
Heterogeneous chemistry	Only reactions on Polar Stratospheric Clouds (stratosphere) yet
Aerosol size distribution	Bins
Inorganic aerosols	Included: ISORROPIA module (Guth et al, 2016)
Secondary organic aerosols	Not implemented in current CAMS version
Aqueous phase chemistry	Aqueous reactions for sulphate production
Dry deposition/sedimentation	Resistance approach (Michou et al., 2004) for gases, (Nho-kim et al., 2005) for aerosol
Mineral dust	Included: see evaluation by Sic et al. (2014)
Sea Salt	Included: see evaluation by Sic et al. (2014)
Boundary values	Values delivered by global CAMS and MOCAGE global domain (2°) for the other chemical species
Initial values	24h forecast from the day before
Anthropogenic emissions	CAMS-REG-AP_v3.1/2016
Biogenic emissions	Fixed monthly biogenic emission, based upon Simpson approach
Forecast system	
Meteorological driver	12:00 UTC operational IFS forecast for the day before
Assimilation system	
Assimilation method	3d-var
Observations	O_3, NO_2 and PM_{10} in-situ data distributed by Meteo-France
Frequency of assimilation	Hourly
Meteorological driver	00:00 UTC operational IFS forecast

7.2 Forward model

The MOCAGE 3D multi-scale Chemistry and Transport Model has been designed for both research and operational applications in the field of environmental modelling. Since 2000, MOCAGE has been allowing to cover a wide range of topical issues ranging from chemical weather forecasting, tracking and backtracking of accidental point source releases, trans-boundary pollution assessment, assimilation of remote sensing measurements of atmospheric composition, to studies of the impact of anthropogenic emissions of pollutants on climate change, with over 60 references in the international refereed literature. For this, the MOCAGE structure offers flexibility to tailor the model CPU/MEM requirements and parameterisations to the different applications. MOCAGE has been running daily since 2005. Meteo-France joined in 2004 the partnership consortium and operational platform 'PREV'AIR' (Rouil et al., 2009), in charge of the pollution monitoring and forecasting over France.

7.2.1 Model geometry

MOCAGE simultaneously considers the troposphere and stratosphere at the planetary scale and over limited-area sub-domains at higher horizontal resolution, the model providing (by default) its own time-dependent chemical boundary conditions. For the CAMS Regional production, the MOCAGE configuration comprises a global domain (2° resolution) and the regional domain (25°W-45°E and 30°N-70°N at 0.1 or 0.2° resolution for respectively forecast and assimilation). The products delivered for the CAMS service are issued from the regional domain only. In the vertical, 47 hybrid (σ, P) levels go from the surface up to 5 hPa, with approximately 8 levels in the Planetary Boundary Layer (i.e. below 2km), 16 in the free troposphere and 24 in the stratosphere. The thickness of the lowest layer is about 40 m.

7.2.2 Forcings and boundary conditions

7.2.2.1 Meteorology

The MOCAGE configuration that has been developed and operated since the MACC project runs in off-line mode, forced by IFS meteorological analyses or forecasts. For the daily forecast production, the IFS daily operational forecasts are used: 0-108h (to cover the 96h forecast time range) 3 hourly forecasts of horizontal winds, humidity and surface pressure are taken from the 12 UTC suite. For the daily analysis production, the same fields are taken from the 00 UTC IFS suite.

7.2.2.2 Chemistry

Chemical initial values in the regional domain are provided by MOCAGE 24h forecast from the day before. The boundary conditions are taken from global CAMS operational suite for the species

(chemical and aerosols) that are distributed (see Table 7). For aerosols, the 2 or 3 bins from C-IFS are summed to get total concentration and then distributed onto the 6 MOCAGE bins considering Mean C-IFS bin size as emission modes. A factor 4.3 is applied to convert Sea Salt from wet to dry fractions. Aerm03 (of diameter larger than 10µm) is only marginally distributed within MOCAGE PM_{10} sea salt because of the matching between bins and log-normal modes. For the other species, the concentrations from the MOCAGE global domain are used, which helps to introduce smoothly, on the horizontal as well as on the vertical, these chemical boundary conditions into the CAMS regional domain.

Table 7. The chemical and aerosol species taken from C-IFS and used in MOCAGE

C-IFS Species	**Coupled to MOCAGE Species**
go3	O_3
CO	CO
SO_2	SO_2
aermr01, aermr02, aermr03	Sea salt (6 bins)
aermr04, aermr05, aermr06	Desert dust (6 bins)
aermr07, aermr08	Organic carbon (6 bins)
aermr09, aermr10	Black carbon (6 bins)

7.2.2.3 Surface emissions

Surface emissions are pre-processed using the SUMO2 pre-processor. Anthropogenic emissions from CAMS-REG-AP_v3.1/2016 are used.

7.2.3 Dynamical core

The dynamical forcings from IFS (hydrostatic winds, temperature, humidity and pressure) feed the advection scheme, as well as the physical and chemical parameterisations. Forcings are read-in every 3 hours, and are linearly interpolated to yield hourly values, which is the time-step for advection; smaller time-steps are used for physical processes and chemistry, but the meteorological variables are kept constant over each hour. MOCAGE is based upon a semi-lagrangian advection scheme (Williamson and Rasch, 1989), using a cubic polynomial interpolation in all 3 directions. Evaluation of transport in MOCAGE using Radon-222 experiments can be found in (Josse et al., 2004).

Concerning physical and chemical parameterisations, an operator splitting approach is used. Parameterisations are called alternatively in forward and reverse order, with the objective to reduce systematic errors.

7.2.4 Physical parameterisations

Several options are available within MOCAGE; we briefly mention here the options used for the CAMS Regional production.

7.2.4.1 Turbulence and convection

For sub-gridscale transport processes, vertical diffusion is treated following Louis (1979) and transport by convection is from Bechtold et al. (2001). Scavenging within convective clouds is following Mari et al. (2000), allowing to compute wet removal processes directly within the convective transport parameterisation. Wet deposition in stratiform clouds and below clouds follows Giorgi and Chameides (1986).

7.2.4.2 Deposition

A description of MOCAGE surface exchanges module is presented in Michou et al. (2004). The dry deposition parameterisation relies on a fairly classical surface resistance approach (Wesely, 1989), but with a refined treatment of the stomatal resistance, similar to the one used in Meteo-France NWP models: see description of the ISBA original approach in (Noilhan and Planton, 1989). Sedimentation of aerosol follows (Nho-Kim et al., 2004).

7.2.5 Chemistry and aerosols

The MOCAGE configuration for CAMS comprises 118 species and over 300 reactions and photolysis. It is a merge of reactions of the RACM scheme (Stockwell et al., 1997) with the reactions relevant to the stratospheric chemistry of REPROBUS (Lefèvre et al., 1994). Aqueous chemistry for the formation of sulphate is represented, following (Ménegoz et al., 2009). Detailed heterogeneous chemistry on Polar Stratospheric Clouds (types I, II) is accounted for, as described in Lefèvre et al. (1994). Other heterogeneous chemistry processes are currently not included.

Photolysis is taken into account using a multi-entry look-up table computed off-line with the TUV software version 4.6 (Madronich, 1987). Photolysis depends on month (including monthly aerosol climatologies), solar zenith angle, ozone column above each cell (as the model extends to the mid-stratosphere, it is actually the ozone profile computed by MOCAGE which is used at every time step), altitude and surface albedo in the UV. They are computed for clear-sky conditions and the impact of cloudiness on photolysis rates is applied afterwards.

The aerosol module of MOCAGE includes the primary species dusts, black carbon, sea salts, organic carbon, and the secondary inorganic species sulfate, nitrate and ammonium. The formation and the multi-phasic equilibrium of inorganic secondary aerosols are modelled by the ISORROPIA-II module. Details on MOCAGE aerosol simulation evaluation can be found in Martet et al. (2009) for dusts, in

Nho-Kim et al. (2005) for black carbon, and in Sic et al. (2015) for the latest version of MOCAGE primary aerosol module. The implementation and the evaluation of secondary inorganic aerosols in MOCAGE are described by Guth et al (2016). Further improvements of the representation of aerosols in MOCAGE are expected in the future with on-going work regarding organic secondary aerosols.

7.3 Assimilation system

Any assimilation algorithm can be seen as a sequence of elementary operations or elementary components that can exchange data (Lagarde et al., 2001). Based on this idea, CERFACS has developed a coupling PALM software (www.cerfacs.fr/~palm) that manages the dynamic launching of the components of assimilation systems (forecast model, algebra operators, I/O of observational data, etc.) and the parallel data exchanges.
MOCAGE operations for CAMS use the assimilation system based upon MOCAGE and PALM, which has been developed and evaluated during the European ASSET project (Lahoz et al., 2007). This system is particularly versatile, as both the CTM degree of sophistication (for instance, the number of chemical tracers involved, the physical or chemical parameterisations, the horizontal and vertical geometries, etc.) and the data assimilation technique used via PALM can be changed easily. Current available options are 3D-VAR, 3D-FGAT and incremental 4D-VAR methods to assimilate profile and column data for key measured atmospheric constituents, by means of a generic observation operator component. As a first approximation, background error standard deviations are prescribed as proportional to background amounts. In order to spread assimilation increments spatially, background error correlations are modelled using a generalized diffusion operator (Weaver and Courtier 2001). Several data assimilation experiments have been published with MOCAGE, both for the stratosphere and troposphere.

Based on past experience, MOCAGE for CAMS uses a 3D-VAR technique, with an assimilation window that is 1h every hour. MOCAGE assimilates O_3, NO_2 and PM_{10} in-situ surface observations for re-analyses and for NRT analyses. The species are assimilated independently every hour without any cross-species covariances, and then the increments per species are added to the analysis that serves at initial condition for computing the background of the next hour of the assimilation process.

8. SILAM factsheet

8.1 Assimilation and forecast system: synthesis of the main characteristics

Assimilation and forecast system	
Horizontal resolution	0.1° regular lat-lon grid
Vertical resolution	69 layers for meteorological pre-processor (IFS hybrid levels 69 to 137, covering the troposphere), 10 layers for chemistry and vertical sub-grid-scale mixing calculations, with layer tops at 25,75,175,375,775,1500,2700,4700,6700 and 8700m above surface
Gas phase chemistry	CBM-4 gas-phase transformation, inorganic chemistry scheme with input to heterogeneous transformations (Sofiev, 2000)
Heterogeneous chemistry	Sofiev (2000)
Aerosol size distribution	Bins. Varies: for anthropogenic source, follows the emission of $PM_{2.5-10}$ split, for sea salt uses 5 bins from 10nm up to 30μm, dust is split into 4 bins from 10nm up to 30 μm
Inorganic aerosols	SO_4, NO_3, NH_4, EC, anthropogenic mineral, sea salt, desert dust
Secondary organic aerosols	Volatility Basis-Set
Aqueous phase chemistry	SO_2 oxidation, nitrate formation (Sofiev, 2000), heterogeneous nitrate formation on sea salt particles
Dry deposition/sedimentation	Resistance approach (Wesely et al., 1989) for gases, (Kouznetsov & Sofiev, 2012) for aerosols
Mineral dust	Taken from the C-IFS boundary conditions
Sea Salt	Updated source term Sofiev et al (2011)
Boundary values	C-IFS values for all available species, except for sea salt, which is taken from SILAM global forecasts
Initial values	24h forecast from the day before
Anthropogenic emissions	CAMS-REG-AP_v3.1/2016
Biogenic emissions	Dynamic biogenic emissions, based upon Poupkou et al. (2010)
Forecast system	
Meteorological driver	12:00 UTC operational IFS forecast for the day before (up to +108)
Assimilation system	
Assimilation method	Operational intermittent 3d-var for analysis; 4dvar for pollen re-analysis

Observations	In-situ surface data O_3, NO_2, $PM_{2.5}$, PM_{10}, SO_2, CO operational; and vertically integrated columns in research mode (NO_2, AOD)
Frequency of assimilation	Hourly
Meteorological driver	00:00 UTC operational IFS forecasts up to +24h

8.2 Forward model

The System for Integrated modeLling of Atmospheric coMposition SILAM v.5.6 (Sofiev et al, 2015) is a Eulerian chemical transport model with the transport module based on advection scheme of Galperin (2000) refined by Sofiev et al (2015) and adaptive vertical diffusion algorithm of Sofiev (2002). Apart from the transport and physico-chemical cores described below, SILAM includes a set of supplementary tools including a meteorological pre-processor, input-output converters, reprojection and interpolation routines, etc. In the operational forecasts, these enabled direct forcing of the model by the ECMWF IFS meteorological fields. A system outlook can also be found at http://silam.fmi.fi.

8.2.1 Model geometry

8.2.1.1 Horizontal computational grid

number of grid cells: nx = 700 ny = 420
western-most longitude = 25.05 W, eastern-most longitude = 44.95° E
southern-most latitude = 30.05 N, northern-most latitude = 71.95° N
resolution: dx = 0.1° dy = 0.1°

8.2.1.2 Vertical grids

Following Sofiev (2002), SILAM uses a multi-vertical approach with the meteorology-resolving grid corresponding to the tropospheric part of the IFS vertical: hybrid levels from 69 to 137. The chemical transformations and vertical fluxes are computed based on 10 thick staggered layers, with the thickness increasing from 25 m for the lowest layer to 1000-2000 m in the free troposphere. Within the thick layers, the sub-grid information is used to evaluate the weighted averages of the high-resolution meteorological parameters and effective diffusion coefficients.

8.2.2 Forcings and boundary conditions

8.2.2.1 Meteorology

Meteorological forcing is the ECMWF IFS operational forecasts taken from the 12UTC forecast of the previous day. Thus, the forecast length of the meteorology fields is from +12 hr till +84 hr. The meteo fields are taken from the operational dissemination procedure of ECMWF in rotated lon-lat coordinates system (southern pole of the rotated grid is at (0E, 30S)) with 0.1° resolution.

8.2.2.2 Chemistry

Boundary conditions are taken from the C-IFS (see Table 8). The full fields are imported every 3 hours; in-between, the linear interpolation is applied. Due to repeated criticism of sea-salt levels of the IFS, the SSA boundary conditions are taken from SILAM own global forecasts.

Table 8. The chemical and aerosol species taken from C-IFS and used in SILAM

C-IFS Species	**Coupled to SILAM Species**	**Comments**
Go_3	O_3	Only GO3 is used by SILAM
CO	CO	
NO	NO	
NO_2	NO_2	
PAN	PAN	
SO_2	SO_2	
C_5H_8	C_5H_8	
C_2H_6	2xPAR	
HNO_3	HNO_3	
Dust	Dust	3 C-IFS bins remapped to 5 SILAM bins
OC hydrophilic aermr07	AVB0	Non-volatile bin of organic aerosol
OC hydrophobic aermr08	AVB0	
BC hydrophilic aermr09	EC	
BC hydrophobic aermr10	EC	
Sulphates aermr 11	Sulphates	1 C-IFS mode split equally to 2 SILAM modes
Aerm01, aerm02	Sea salt	C-IFS Sea salt divided by 4.3 for conversion from wet to dry mass

8.2.2.3 Surface emissions

Emission fields are based on the CAMS-REG-AP_v3.1/2016 database for CO, SO_2, NO_x, NH_3, NMVOC, $PM_{2.5}$ and $PM_{2.5-10}$, for reference year 2015. The $PM_{2.5}$ emissions are split into EC, OC and mineral components, and OC is mapped to the volatility bins according to Shrivastava et al.(2011). Emissions of biogenic VOCs and sea salt are computed in the corresponding SILAM dynamic modules, which are described below. GFAS hourly emissions from wild-land fires are replicated from D-2 to D+1 for forecast and shut down after, for analysis mode used as is.

8.2.3 Transport core

The SILAM Eulerian transport core (Sofiev et al, 2015) is based on the coupled developments: refined advection scheme of Galperin (2000) and vertical diffusion algorithm of Sofiev (2002) and Kouznetsov & Sofiev (2012). The methods are compatible, in a sense that both use the same set of variables to determine the sub-grid distribution of tracer mass. The approach, in particular, allows computing correct vertical exchange using high-resolution input data but low-resolution chemistry and diffusion grids. The later feature is used in the vertical setup with 9 thick layers.

8.2.4 Physical parameterisations

8.2.4.1 Turbulence and convection

Diffusion is parameterised following the first-order K-theory based closure. Horizontal diffusion is embedded into the advection routine, which itself has zero numerical viscosity, thus allowing full control over the diffusion fluxes. The vertical diffusivity parameterisation follows the approach suggested by Genikhovich et al. (2004), as described in Sofiev et al (2010). The procedure diagnoses all the similarity theory parameters using the profiles of the basic meteorological quantities: wind, temperature and humidity. Output includes the value of eddy diffusivity for scalars at some reference height (taken to be 1m).

8.2.4.2 Deposition

Dry deposition parameterisation follows the standard resistive analogy of Wesely (1989). Deposition velocity for aerosols are evaluated using the original (Kouznetsov & Sofiev, 2012) algorithm. Wet deposition parameterisation is based on the scavenging coefficient after Sofiev (2000) for gas species and a new deposition scheme for aerosols following the generalised formulations of (Kouznetsov & Sofiev, 2012).

8.2.5 Chemistry and aerosols

The main gas-phase chemical mechanism is CBM-4. The heterogeneous scheme is an updated version of the DMAT model scheme (Sofiev, 2000). It incorporates the formation pathways of secondary inorganic aerosols.

Emission of 2 sets of compounds is embedded into the simulations: biogenic VOC, sea salt, and desert dust. The bio-VOC computations follow the Poupkou et al. (2010) model and provide isoprene and mono-terpene emissions (currently, only isoprene emission is used in the CB-4 mechanism). The sea salt emission parameterisation is the original development generally based on Sofiev et al (2011), with refinements and spume formation mechanism added in v5.2.

8.3 Assimilation system

The embedded data assimilation is based on the 3- and 4-dimensional variational approach (3D-, 4D-VAR, Vira & Sofiev, 2012, 2015). The adjoint formulations exist for all dynamic modules, linearized transformation scheme of sulphur oxide and for aerosol particles. The assimilation procedure has been tested for both initialising the concentration fields and for refinement of the emission coefficients. The observation operators exist for in-situ observations and for the vertically integrated columns observed by the nadir-looking satellites.

For the near-real time analyses, the previous-day observations are used in a 3D-VAR data assimilation suite. The assimilated species are NO_2, O_3 and $PM_{2.5}$, PM_{10}, SO_2 and CO.

9. DEHM factsheet

9.1 Assimilation and forecast system: synthesis of the main characteristics

Assimilation and forecast system	
Horizontal resolution	18 km at 60°N
Vertical resolution	29 vertical layers using terrain-following σ-coordinates from the surface up to 100 hPa. Lowest layer extends from the surface to about 23 m. Approximately 12 layers within the lowest 1000 m of the atmosphere.
Gas phase chemistry	A modified version of the Strand and Hov (1994) scheme, including an improved description of e.g. transformations of nitrogen containing compounds
Heterogeneous chemistry	Rates based on NH_3-HNO_3-NH_4NO_3 equilibrium and NH_3-H_2SO_4-SO_4 rates. Oxidation of NO_2 by O_3 on aerosols
Aerosol size distribution	2 size fractions: $PM_{2.5}$ and coarse fraction of PM_{10}
Inorganic aerosols	Sulphate, Nitrate and Ammonium
Secondary organic aerosols	Based on a VBS approach as described in Bergström et al, 2012 ("NPAS" scheme i.e. no partitioning of POA, aging of SOA)
Aqueous phase chemistry	SO_2 oxidation by O_3 and H_2O_2 (Jonson et., 2000)
Dry deposition/sedimentation	Gaseous and aerosol dry-deposition velocities are calculated based on the resistance method
Mineral dust	Apart from anthropogenic dust, also natural dust is read in at the lateral boundaries (from C-IFS) and transported within the domain
Sea Salt	In 2 size bins
Boundary values	C-IFS forecasts (global CAMS product)
Initial values	Previous forecast
Anthropogenic emissions	CAMS-REG-AP_v3.1/2016
Biogenic emissions	Isoprene and monoterpenes
Forecast system	
Meteorological driver	12:00 UTC operational IFS forecast for the day before
Assimilation system	
Assimilation method	Optimal interpolation
In-situ observations	O_3 and NO_2 provided by INERIS (rural sites)
Frequency of assimilation	At every full hour during 8:00-19:00 UTC

Satellite observations	None
Meteorological driver	operational IFS forecast and analyses for the same day (0.2°, 45 levels)

9.2 Forward model

The Danish Eulerian Hemispheric Model (DEHM) is a 3-dimensional, offline, large-scale, Eulerian, atmospheric chemistry transport model (CTM) developed to study long-range transport of air pollution in the Northern Hemisphere. DEHM was originally developed in the early 1990's in our modelling group in order to study the atmospheric transport of sulphur-dioxide and sulphate into the Arctic (Christensen, 1997; Heidam et al., 1999; Heidam et al., 2004). The model has been modified, extended and updated continuously since then. The original simple sulphur-dioxide-sulphate chemistry has been replaced by a more comprehensive chemical scheme, including 73 chemical species, 9 primary particles and 158 chemical reactions.

9.2.1 Model geometry

The model domain used in previous studies covers most of the Northern Hemisphere, discretized on a polar stereographic projection, and includes a 2-way nesting procedure with several nests – currently up to 3 – with higher resolution over Europe, Northern Europe and Denmark. Currently the finest resolution is 5.56 km x 5.56 km for a domain covering Denmark. The vertical discretization is defined on an irregular grid with 29 layers up to ~18 km. The thickness of the lowest layer is 15–25 m. However, the definition of both the horizontal and vertical discretization is flexible and can be changed according to the applied meteorology.
Within CAMS_50, DEHM is set up with a domain including the CAMS_50 area: 25°W to 45°E and 30°N to 70°N, with an average resolution of ca. 18 km. In the coming year we will make analysis of how we can increase the resolution in order to go towards 0.1 dg. The applied DEHM domain can be seen in Figure 3, where the standard CAMS_50 domain is indicated by the blue lines.

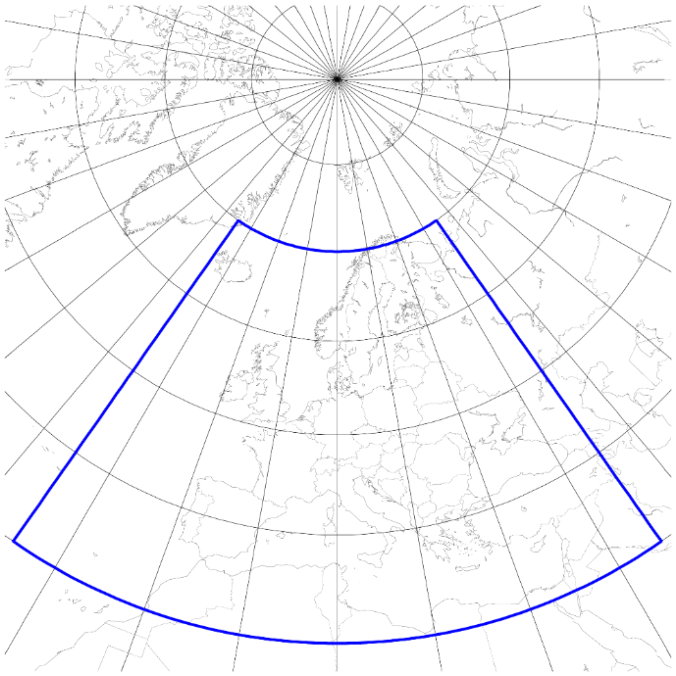

Figure 3 - The new DEHM domain and indicated by the blue lines the standard CAMS_50 domain where output is required.

9.2.2 Forcings and boundary conditions

9.2.2.1 Meteorology

The forcing meteorology is retrieved from the IFS model system on a 0.2°x0.2° horizontal grid/45 vertical levels and with a temporal resolution of 3 hours. The meteorological data are interpolated in time and to the applied spatial grid.

9.2.2.2 Chemistry and aerosols

DEHM is initialised with the C-IFS forecasts (global CAMS product) in the first initial run. Thereafter, depending on how the forecast should be set up, e.g. each daily forecast can be initialised by using the 3-d concentrations field from the DEHM-forecast at the 24-hour forecast time from the previous forecast the day before. The chemical boundary condition for each forecast are obtained from the C-IFS forecasts starting e.g. the day before (T+24) with a 3-hour time step. The C-IFS fields included in DEHM are given in Table 9. Most of the species are linked directly to the same species in DEHM. However, it should be noted that the bins in C-IFS are not completely aligned with the 2 bins in DEHM (where fine is $PM_{2.5}$ and coarse is the non-$PM_{2.5}$ part of PM_{10}).

Table 9. The chemical and aerosol species taken from C-IFS and used in DEHM (updated).

C-IFS Species	**Coupled to DEHM Species**
GO_3	O_3
CO	CO
NO	NO
NO_2	NO_2
PAN	PAN
HNO_3	HNO_3
HCHO	HCHO
SO_2	SO_2
C_2H_6	C_2H_6
C_3H_8	goes into DEHMs group of higher alkenes
C_5H_8	C_5H_8
Sea Salt fine (aermr01: Sea Salt bin1 (0.03 - 0.5 um))	Sea Salt fine
Sea Salt coarse (aermr02: Sea Salt bin2 (0.5 - 5 um))	Sea Salt coarse
BCfresh (aermr09)	BCfresh (all in fine fraction)
BCaged (aermr10)	BCaged (all in fine fraction)
SO_4 (aermr11)	SO_4
dust_aermr04 (Dust Aerosol bin 1 (0.03 - 0.55 um)	fine dust fraction
dust_aermr05 (Dust Aerosol bin2 (0.55 - 0.9 um)	fine dust fraction
dust_aermr06 Dust Aerosol bin 3 (0.9 - 20 um)	coarse dust fraction

The link between SS and dust in the coarse and fine fraction:

SS_2.5=SS1/4.3 + 0.5 * SS2/4.3
Coarse SS = 0.5 * SS2/4.3 (as this is only the non-PM2.5 part).

Dust_2.5= dust_aermr04 + dust_aermr05
Dust_coarse= 0.4* dust_aermr06

9.2.2.3 Surface emissions

The current operational version include the CAMS-REG-AP_v3.1/2016 anthropogenic emissions, but the model code has also been modified in order to include the GFAS biomass burning emission. Standard temporal profiles for the various SNAP sectors are applied based on profiles from the Eurodelta project.

Natural emissions of the Biogenic Volatile Organic Compounds (BVOCs) isoprene and monoterpenes are estimated in the DEHM model based on the MEGAN model (see Zara et al. 2012 for details). The production of sea salt aerosols at the ocean surface is based on 2 parameterisation schemes describing the bubble-mediated sea spray production of smaller and larger aerosols. In each time step, the production is calculated for 10 size bins and thereafter summed up to give an aggregated production of fine (with dry diameters <1.3 um) and coarse (with dry diameters ranging 1.3-6um) aerosols (see Soares et al. 2016 for details).

9.2.3 Dynamical core

The horizontal advection is solved numerically using the higher order Accurate Space Derivatives scheme, documented to be very accurate (Dabdub and Seinfeld, 1994), especially when implemented in combination with a Forester filter (Forester, 1977). The vertical advection as well as the dispersion sub-models is solved using a finite elements scheme (Pepper et al., 1979) for the spatial discretization. For the temporal integration of the dispersion, the q-method (Lambert, 1991) is applied and the temporal integration of the 3 dimensional advection is carried out using a Taylor series expansion to third order. Time integration of the advection is controlled by the Courant-Friedrich-Lewy (CFL) stability criterion. An adjustment of the horizontal winds is included in order to ensure mass conservation.

9.2.4 Physical parameterisations

9.2.4.1 Turbulence and convection

The vertical diffusion is configured by Kz profiles (Hertel et al., 1995), based on Monin-Obukhov similarity theory (see, e.g. Seinfeld, 1986) for the surface layer. This Kz profile is extended to the whole boundary layer by using a simple extrapolation, which ensures that Kz is decreasing in the upper part of the boundary layer. The planetary boundary layer (PBL) height is obtained directly from the IFS meteorology.

9.2.4.2 Deposition

Gaseous and aerosol dry-deposition velocities are calculated based on the resistance method and are configured similar to the EMEP model (Simpson et al., 2003; Emberson et al., 2000), except for the dry deposition of species on water surfaces, where the deposition depends on the solubility of the chemical species and the wind speed (Hertel et al., 1995).
Wet deposition includes in-cloud and below-cloud scavenging and is calculated as the product of scavenging coefficients and the concentration of gases and particles in air. The in-cloud scavenging coefficients are dependent on Henry's law constants and the rate at which precipitation is formed.

9.2.5 Chemistry and aerosols

9.2.5.1 Chemistry

The basic chemical scheme in DEHM includes 74 different species and is based on the scheme by Strand and Hov (1994), but with some additions (see below). The current model describes concentration fields of 74 photo-chemical compounds (including NOx, SOx, VOC, NHx, CO, etc.). A total of 158 chemical reactions are included. Furthermore, the model has options for an additional chemical scheme for mercury (Hg) and a module for emissions and transport of persistent organic pollutants (POPs), including an extensive description of air-surface exchange of POPs for soil, water, vegetation and snow.

9.2.5.2 Aerosol

The original Strand and Hov scheme has been modified in order to improve the description of, amongst other things, the transformations of nitrogen containing compounds. The chemical scheme has been extended with a detailed description of the ammonia chemistry through the inclusion of ammonia (NH_3) and related species: ammonium-nitrate (NH_4NO_3), ammonium bisulphate (NH_4HSO_4), ammonium sulphate ($(NH_4)_2SO_4$) and particulate nitrate (NO_3) formed from nitric acid (HNO_3) using an aerosol equilibrium approach with reaction rates dependent on the equilibrium (Frohn, 2004). Furthermore, reactions concerning the wet-phase production of particulate sulphate have been included. The photolysis rates are calculated by using a 2-stream version of the Phodis model (Kylling et al., 1995). The original rates for inorganic and organic chemistry have been updated with rates from the chemical scheme applied in the EMEP model (Simpson et al., 2003). The scheme now contains 9 classes of particulate matter ($PM_{2.5}$, PM_{10}, TSP, seasalt< 2.5 mm, sea-salt >2.5 mm, smoke from wood stoves, fresh black carbon, aged black carbon, and organic carbon). A VBS-based approach for SOA formation has been added as part of CAMS_50 (Zare et al. 2014; Bergström et al., 2012).

9.3 Assimilation system

The data assimilation scheme in DEHM is an optimal interpolation algorithm (Frydendall et al., 2009; Silver et al., 2013). O_3 and NO_2 are assimilated based on in-situ observations at every full hour during 8:00 – 19:00 UTC. The assimilation routine includes at this point observation from stations categorized as background rural, background rural-regional and background rural-remote.

10. GEM-AQ factsheet

10.1 Assimilation and forecast system: synthesis of the main characteristics

Assimilation and forecast system	
Horizontal resolution	0.1° x 0.1° latitude/longitude spherical grid
Vertical resolution	28 vertical levels up to 10 hPa. Hybrid- sigma coordinate system. 14 levels in the bottom 5km.
Gas phase chemistry	Modified ADOM IIB mechanism
Heterogeneous chemistry	Hydrolysis of N_2O_5
Aerosol size distribution	12 size bins
Inorganic aerosols	Sulphates, Nitrates
Secondary organic aerosols	Primary BC + OC and coagulation of OC
Aqueous phase chemistry	SO_2
Dry deposition/sedimentation	Gaseous species - 'big leaf' multiple resistance model (Weswely, 1989; Zhang et al., 2002); Particles – calculation of gravitational settling velocities on-line.
Mineral dust	On-line (Marticorena and Bergametti, 1995)
Sea Salt	On-line Gong-Monahan (Gong, 2003b)
Boundary values	C-IFS
Initial values	Previous day forecast from GEM-AQ
Anthropogenic emissions	CAMS-REG-AP_3.1
Biogenic emissions	MEGAN-MACC
Pollens	Birch, olive
Assimilation module	Optimal Interpolation
Observations	NRT in-situ observations (O_3, NO_2, CO, SO_2, PM_{10}, $PM_{2.5}$) distributed by Meteo-France
Frequency of assimilation	Hourly, performed once a day for the previous day
Forecast system	
Meteorological driver	12:00 UTC operational IFS forecast for the day before. The IFS data are used as boundary conditions with nesting interval of 3 hours. The extent of the piloting is shown in Figure 4.

10.2 Forward model

The GEM-AQ is an on-line chemical weather forecasting model (Kaminski et al., 2008).

10.2.1 Model geometry

The model can be configured to simulate atmospheric processes over a broad range of scales, from the global scale down to the meso-gamma scale. An arbitrarily rotated latitude-longitude mesh focuses resolution on any part of the globe. In the vertical, GEM uses the generalised sigma vertical coordinate system. It has terrain-following sigma surfaces near the ground that transform to pressure surfaces higher in the atmosphere. The model top is set at 10 hPa.

For this phase of the project, the model is run in the limited area mode (LAM) with a resolution of 0.1° x 0.1° on a spherical coordinate system. The extent of the model grid is shown in Figure 4.

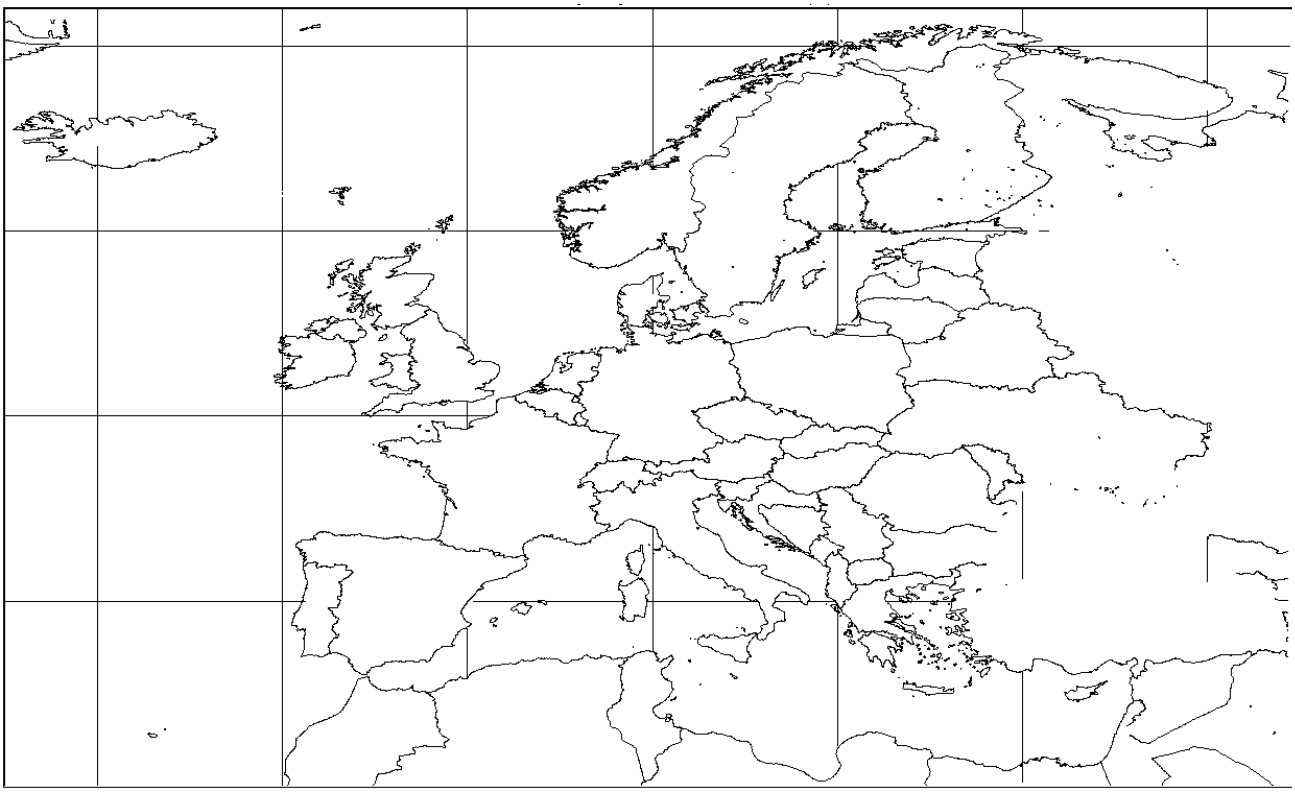

Figure 4 - GEM-AQ domain on a spherical coordinate system.

10.2.2 Forcings and boundary conditions

10.2.2.1 Meteorology

The operational IFS model provides meteorological fields for initial and boundary conditions used by the GEM-AQ model. The GEM-AQ model is started using the 12-hour forecast (valid at 00 UT of the following day) as initial conditions. The IFS data are used as boundary conditions with nesting interval of 3 hours. The IFS meteorological fields are computed from spectral coefficients for the target GEM-

AQ grid. Meteorological fields, within the GEM-AQ model domain, are constrained and relaxed to the IFS global model every 3 hours. Thus, the meteorological fields are 'dynamically interpolated' by the GEM meteorological model to the required transport and chemistry time steps.

10.2.2.2 Chemistry and aerosols

The C-IFS chemical fields are used as boundary conditions with nesting interval of 3 hours starting with the 24-hour forecast. The chemical and aerosol fields taken from C-IFS and used in GEM-AQ are listed in Table 10.

Table 10. The chemical and aerosol fields taken from C-IFS and used in GEM-AQ.

C-IFS Gas Phase Species	**GEM-AQ Gas Phase Species**
NO_2	NO_2
CO	CO
HCHO	HCHO
GO_3	O_3
NO	NO
HNO_3	HNO_3
PAN	PAN
CH_2H_6	CH_2H_6
CH_3H_8	CH_3H_8
CH_4	CH_4
SO_2	SO_2

C-IFS aerosol species	**GEM-AQ aerosol species (mapping of aerosol bins in Table 11 and Table 12)**
aermr04 - Dust Aerosol (0.03 - 0.55 um)	Mineral dust – distributed into 12 bins
aermr05 - Dust Aerosol (0.55 - 0.9 um)	
aermr06 - Dust Aerosol (0.9 - 20 um)	
aermr07 -Hydrophobic Organic Matter Aerosol	Organic carbon – distributed into 12 bins
aermr08 - Hydrophilic Organic Matter Aerosol	
aermr09 - Hydrophobic Black Carbon Aerosol	Black carbon – distributed into 12 bins
aermr10 - Hydrophilic Black Carbon Aerosol	
aermr11 -Sulphate Aerosol	Sulphate – distributed into 12 bins
Sea salt	Computed in the aerosol module in the GEM-AQ model

Table 11 shows mapping of C-IFS aerosol species to the GEM-AQ size bins (percentage) for mineral dust.

Table 11. Mapping of C-IFS aerosol species to the GEM-AQ size bins (percentage) for mineral dust.

GEM-AQ aerosol radius	**low**	0.005	0.01	0.02	0.04	0.08	0.16	0.32	0.64	1.28	2.56	5.12	10.24
	up	0.01	0.02	0.04	0.08	0.16	0.32	0.64	1.28	2.56	5.12	10.24	20.48
	average	0.0075	0.015	0.03	0.06	0.12	0.24	0.48	0.96	1.92	3.84	7.68	15.36
cams Dust aerosol mapping [%]		0	0	20	20	20	20	20	100	25	25	25	25
CAMS Dust Aerosol naming convention		-	-	aermr04 (0.03 - 0.55 um)					aermr05 (0.55 - 0.9 um)	aermr06 -(0.9 - 20 um)			

For organic matter aerosol, black carbon and sulphates the same log-normal based profile was applied. For organic aerosol and black carbon hydrophobic and hydrophilic components were summed as “total organic aerosol” and “total black carbon aerosol” before applying size-bin distribution profiles.

Table 12. Mapping of C-IFS aerosol species to the GEM-AQ size bins (percentage) for organic aerosol, black carbon and sulphates.

GEM-AQ aerosol radius	**lower**	0.005	0.01	0.02	0.04	0.08	0.16	0.32	0.64	1.28	2.56	5.12	10.24
	upper	0.01	0.02	0.04	0.08	0.16	0.32	0.64	1.28	2.56	5.12	10.24	20.48
	average	0.0075	0.015	0.03	0.06	0.12	0.24	0.48	0.96	1.92	3.84	7.68	15.36
Organic Mater = aermr07 + aermr08		8.0	12.3	16.1	17.8	16.5	12.8	8.5	4.5	2.1	1.0	0.3	0.1
Black Carbon = aermr09 + aermr10		8.0	12.3	16.1	17.8	16.5	12.8	8.5	4.5	2.1	1.0	0.3	0.1
Sulphates		8.0	12.3	16.1	17.8	16.5	12.8	8.5	4.5	2.1	1.0	0.3	0.1

10.2.2.3 Surface emissions

For the requested operational set-up, the anthropogenic emissions prepared in the frame of CAMS-REG-AP_v3.1/2016 were used.

Anthropogenic emissions included primary gaseous and particle pollutants for individual GNFR (standardised nomenclature for air pollutants) sectors. The following fields were used: SO_2, NOx, CO, NMVOC, NH_3, PM_{10} and $PM_{2.5}$. Based on this information, emission fluxes for 15 gaseous species (9 hydrocarbons and 6 inorganics) and 4 aerosol components (primary organic aerosol, black carbon, sulphates, nitrates) were derived. Total emission flux for each aerosol component was distributed into 12 bins in the GEM-AQ aerosol module.

Anthropogenic emissions were distributed within the 4 lowest model layers (up to 630 m) with different injection height profiles for each of the SNAP sectors (converted from GNFR according to the guidelines from CAMS_81). Temporal profiles modulating annual and diurnal variation of emission fluxes for each SNAP were used, based on prescribed or averaged GNFR profiles. Anthropogenic emissions outside the area provided by CAMS_81 were compiled using ECLIPSE_v4 (excluding aviation emissions). We plan to consider using CAMS-GLO-ANT and test before U2.

For biogenic emissions, monthly averaged MEGAN-MACC dataset valid for 2010 was used in order to avoid short-term variability of reactive biogenic VOC generated on-line in the model.

Surface anthropogenic and biogenic emission fluxes were applied as a bottom boundary condition in the vertical diffusion equation.

10.2.3 Dynamical core

The set of non-hydrostatic Eulerian equations (with a switch to revert to the hydrostatic primitive equations) maintains the model's dynamical validity right down to the meso-gamma scales. The time discretization of the model dynamics is fully implicit, 2 time-level (Côté et al., 1998ab). The spatial discretization for the adjustment step employs a staggered Arakawa C grid that is spatially offset by half a mesh length in the meridional direction. It is second order accurate, whereas the interpolations for the semi-Lagrangian advection are of fourth-order accuracy, except for the trajectory estimation (Yeh et al., 2002).

10.2.4 Physical parameterisations

10.2.4.1 Turbulence and convection

Deep convective processes are handled by Kain-Fritch convection parameterisation (Kain and Fritch, 1990). The vertical diffusion of momentum, heat and tracers is a fully implicit scheme based on turbulent kinetic energy (TKE) theory.

10.2.4.2 Deposition

The effects of dry deposition are included as a flux boundary condition in the vertical diffusion equation. Dry deposition velocities are calculated from a `big leaf' multiple resistance model (Wesely, 1989; Zhang et al., 2002) with aerodynamic, quasi-laminar layer, and surface resistances acting in series. The process assumes 15 land-use types and takes snow cover into account.

10.2.5 Chemistry and aerosols

10.2.5.1 Chemistry

The gas-phase chemistry mechanism currently used in the GEM-AQ model is based on a modification of version 2 of the Acid Deposition and Oxidants Model (ADOM) Venkatram et al. (1988), derived from the condensed mechanism of Lurmann (1986). The ADOM-II mechanism comprises 47 species, 98 chemical reactions and 16 photolysis reactions. In order to account for background tropospheric chemistry, 4 species (CH_3OOH, CH_3OH, CH_3O_2, and CH_3CO_3H) and 22 reactions were added. All species are solved using a mass-conserving implicit time stepping discretization, with the solution obtained using Newton's method. Heterogeneous hydrolysis of N_2O_5 is calculated using the on-line distribution of aerosol. Although the model meteorology is calculated up to 10 hPa, the focus of the chemistry is in the troposphere where all species are transported throughout the domain. To avoid the overhead of stratospheric chemistry in this version (a combined stratospheric/tropospheric chemical scheme is currently being developed), we replaced both the ozone and NOy fields with climatology above 100 hPa after each transport time step. Ozone fields are taken from the HALOE (Halogen Occultation Experiment) climatology (e.g. Hervig et al., 1993), while NOy fields are taken from the CMAM (Canadian Middle Atmosphere Model). Photolysis rates (J values) are calculated on-line every chemical time step using the method of Landgraf and Crutzen (1998). In this method, radiative transfer calculations are done using a delta-two stream approximation for 8 spectral intervals in the UV and visible applying pre-calculated effective absorption cross sections. This method also allows for scattering by cloud droplets and for clouds to be presented over a fraction of a grid cell. The host meteorological model provides both, cloud cover and water content. The J value package used was developed for MESSy (Joeckel et al., 2006) and is implemented in GEM-AQ.

10.2.5.2 Aerosol

The current version of GEM-AQ has 5 size-resolved aerosols' types, viz. sea salt, sulphate, black carbon, organic carbon and dust as well as nitrates. The microphysical processes that describe formation and transformation of aerosols are calculated by a sectional aerosol module (Gong et al., 2003). The particle mass is distributed into 12 logarithmically spaced bins from 0.005 to 10.24-micron radius. This size distribution leads to an additional 60 advected tracers. The following aerosol processes are accounted for in the aerosol module: nucleation, condensation, coagulation,

sedimentation and dry deposition, in-cloud oxidation of SO_2, in-cloud scavenging, and below-cloud scavenging by rain and snow.

10.3 Assimilation system

Data assimilation in the GEM-AQ modelling system is done with Optimal Interpolation method (i.e. Robichaud and Ménard, 2014) and is applied to the forecast. Error statistics are computed with the Hollingswoth - Lönnberg (HL) method (Hollingswoth and Lonnberg, 1986). The HL method was originally developed for the optimum interpolation method by Rutherford (1972) and refined by Hollingsworth and Lönnberg. It estimates the correlation length and the ratio of observation to model error variances by a least-square fit of a correlation model against the sample of the spatial autocorrelation of observation-minus-model residuals.

Currently, data assimilation is done at each forecast hour for O_3, NO_2, PM_{10} and $PM_{2.5}$, using surface observations provided by Meteo-France for the day before.

11. References

11.1 ENSEMBLE

Galmarini, S., R. Bianco, R. Addis, S. Andronopoulos, P. Astrup, J. C. Bartzis, R. Bellasio, R. Buckley, H. Champion, M. Chino, R. D'Amours, E. Davakis, H. Eleveld, H. Glaab, A. Manning, T. Mikkelsen, U. Pechinger, E. Polreich, M. Prodanova, H. Slaper, D. Syrakov, H. Terada and L. Van der Auwera, 2004. Ensemble dispersion forecasting - Part II: application and evaluation, *Atmospheric Environment*, 38, 28, 4619 – 4632.

Marécal, V., V.-H. Peuch, C. Andersson, S. Andersson, J. Arteta, M. Beekmann, A. Benedictow, R. Bergström, B. Bessagnet, A. Cansado, F. Chéroux, A. Colette, A. Coman, R. L. Curier, H. A. C. Denier van der Gon, A. Drouin, H. Elbern, E. Emili, R. J. Engelen, H. J. Eskes, G. Foret, E. Friese, M. Gauss, C. Giannaros, J. Guth, M. Joly, E. Jaumouillé, B. Josse, N. Kadygrov, J. W. Kaiser, K. Krajsek, J. Kuenen, U. Kumar, N. Liora, E. Lopez, L. Malherbe, I. Martinez, D. Melas, F. Meleux, L. Menut, P. Moinat, T. Morales, J. Parmentier, A. Piacentini, M. Plu, A. Poupkou, S. Queguiner, L. Robertson, L. Rouïl, M. Schaap, A. Segers, M. Sofiev, L. Tarasson, M. Thomas, R. Timmermans, A. Valdebenito, P. van Velthoven, R. van Versendaal, J. Vira, and A. Ung, 2015. A regional air quality forecasting system over Europe: the MACC-II daily ensemble production, *Geosci. Model Dev.*, 8, 2777-2813.

Riccio, A., G. Giunta and S. Galmarini, 2007. Seeking for the rational basis of the Median Model: the optimal combination of multi-model results, *Atmos. Chem. Phys.*, 7, 6085—6098.

Sofiev, M., Ritenberga, O., Albertini, R., Arteta, J., Belmonte, J., Bonini, M., Celenk, S., Damialis, A., Douros, J., Elbern, H., Friese, E., Galan, C., Gilles, O., Hrga, I., Kouznetsov, R., Krajsek, K., Parmentier, J., Plu, M., Prank, M., Robertson, L., Steensen, B. M., Thibaudon, M., Segers, A., Stepanovich, B., Valdebenito, A. M., Vira, J., and Vokou, D., 2017: Multi-model ensemble simulations of olive pollen distribution in Europe in 2014, *Atmos. Chem. Phys.* Discuss., doi:10.5194/acp-2016-1189, in review.

Tukey, J., *Exploratory Data Analysis*, Addison-Wesley, 1977, pp. 43-44.

Wilks, D. S., 2015. Statistical Methods in the Atmospheric Sciences: an introduction, 2nd Edition, *Academic Press*, pp 627.

Denier van der Gon, H. A. C., Bergström, R., Fountoukis, C., Johansson, C., Pandis, S. N., Simpson, D., and Visschedijk, A. J. H.: Particulate emissions from residential wood combustion in Europe – revised estimates and an evaluation, *Atmos. Chem. Phys.*, 15, 6503-6519, 10.5194/acp-15-6503-2015, 2015.
EMEP: Status Report, MSCW/CEIP/CCC, 2019.

TFEIP/TFMM: Improving Emissions of Condensable Particulate Matter in the Context of the LRTAP Convention, EMEP TFEIP/TFMM 2018.

11.2 CHIMERE

Beekmann M., and Derognat C.: Monte Carlo uncertainty analysis of a regional-scale transport chemistry model constrained by measurements from the atmospheric pollution over the Paris area (ESQUIF) campaign, *J. Geophys. Res.*, 108(D17), 8559, doi:10.1029/2003JD003391, 2003.

Bessagnet B., L. Menut, G. Aymoz, H. Chepfer and R. Vautard, Modelling dust emissions and transport within Europe: the Ukraine March 2007 event, *J. Geophys. Res.*, 113, D15202, doi:10.1029/2007JD009541, 2008.

Bessagnet B., L.Menut, G.Curci, A.Hodzic, B.Guillaume, C.Liousse, S.Moukhtar, B.Pun, C.Seigneur, M.Schulz, Regional modeling of carbonaceous aerosols over Europe - Focus on Secondary Organic Aerosols, *J. Atmos. Chem.*, in press, 2009.

Boynard, A., Beekmann, M., Foret, G., Ung, A., Szopa, S., Schmechtig, C. and Coman, A.: Assessment of regional ozone model uncertainty with a modelling ensemble using an explicit error representation, *Atm. Env.*, 45, 784-793, 2011.

Coman, A., Foret, G., Beekmann, M., Eremenko, M., Dufour, G., Gaubert, B., Ung, A., Schmechtig, C., Flaud, J.-M., and G. Bergametti, Assimilation of IASI partial tropospheric columns with an Ensemble Kalman Filter over Europe, 26943-26997, 11, *ACPD*, 2011.

Ebel, A., Friedrich, R., and Rodhe, H. (1994). Tropospheric modelling and emission estimation: Generation of european emission data for episodes (genemis) project, eurotrac annual report 1993, part 5.

Eremenko, M., Dufour, G., Foret, G., Keim, C., Orphal, J., Beekmann, M., Bergametti, G., and Flaud, J.-M.: Tropospheric ozone distributions over Europe during the heat wave in July 2007 observed from infrared nadir spectra recorded by IASI, *Geophys. Res. Lett.*, 35, L18805,doi:10.1029/2008GL034803, 2008.

Evensen, G., Sequential data assimilation with a nonlinear quasigeostrophic model using Monte Carlo methods to forecast error statistics, *J. Geophys. Res.*, 99 (C5), 10143-10162, 1994.

Flemming, J., van Loon, M., Stern, R., 2004. Data assimilation for CTM based on optimum interpolation and KALMAN filter. In: Borrego, C., Incecik, S. (Eds.), *Air Pollution Modeling and its Application*, vol. XVI. Kluwer Academic/Plenum Publishers, New York.

Flemming, J., A., Inness, H., Flentje, V., Huijnen, P., Moinat, M. G., Schultz, and O. Stein, Coupling global chemistry transport models to ECMWF's integrated forecast system, *Geosci. Model Dev.*, 2, 253-265, 2009.

Guenther, A., Karl, T., Harley, P., Wiedinmyer, C., Palmer, P.I. and Geron, C.: Estimates of global terrestrial isoprene emissions using MEGAN (Model of Emissions of Gases and Aerosols from Nature), *Atmos. Chem. Phys.*, 6, 3181-3210, 2006.

Hanea, R., Velders, G. and Heemink, Data assimilation of ground level ozone in Europe with a Kalman filter and chemistry transport model, *J. Geophys. Res.*, 109, 5183-5198, 2004.

Mailler S., L. Menut, D. Khvorostyanov, M. Valari, F. Couvidat, G. Siour, S. Turquety, R. Briant, P. Tuccella, B. Bessagnet, A. Colette, L. Letinois, and F. Meleux, CHIMERE-2017: from urban to hemispheric chemistry-transport modeling , *Geosci. Model Dev.*, 10, 2397-2423, https://doi.org/10.5194/gmd-10-2397-2017.

Mailler, S., Khvorostyanov, D. and Menut, L. (2013). Impact of the vertical emission profiles on ground-level gas-phase pollution simulated from the EMEP emissions over Europe. Atmos Chem Phys, 13:5987–5998.

Menut, L., Goussebaile, A., Bessagnet, B., Khvorostiyanov, D. and Ung, A. Impact of realistic hourly emissions profiles on air pollutants concentrations modelled with CHIMERE, Atmospheric Environment, Volume 49, 2012, Pages 233-244.

Menut L, B.Bessagnet, D.Khvorostyanov, M.Beekmann, N.Blond, A.Colette, I.Coll, G.Curci, G.Foret, A.Hodzic, S.Mailler, F.Meleux, J.L.Monge, I.Pison, G.Siour, S.Turquety, M.Valari, R.Vautard and M.G.Vivanco, 2013, CHIMERE 2013: a model for regional atmospheric composition modelling, *Geoscientific Model Development*, 6, 981-1028.

Menut, L., Flamant, C., Turquety, S., Deroubaix, A., Chazette, P., and Meynadier, R.: Impact of biomass burning on pollutant surface concentrations in megacities of the Gulf of Guinea, Atmos. Chem. Phys., 18, 2687-2707, https://doi.org/10.5194/acp-18-2687-2018, 2018.

Laurent Menut, Arnaud Goussebaile, Bertrand Bessagnet, Dmitry Khvorostiyanov, Anthony Ung, Impact of realistic hourly emissions profiles on air pollutants concentrations modelled with CHIMERE, Atmospheric Environment, Volume 49, 2012, Pages 233-244.

Passant, N. (2002). Speciation of uk emissions of nmvoc. (AEAT/ENV/R/0545).
Terrenoire, E., Bessagnet, B., Rouïl, L., Tognet, F., Pirovano, G., Létinois, L., Beauchamp, M., Colette, A., Thunis, P., Amann, M. and Menut, L. (2015). High-resolution air quality simulation over Europe with the chemistry transport model CHIMERE. Geoscientific Model Development, 8(1):21–42

Rouïl L., et al, PREV'AIR: an operational forecasting and mapping system for air quality in Europe, Bull. *Am. Meteor. Soc.*, doi: 10.1175/2008BAMS2390.1, 2009.
Szopa S., G. Foret, L. Menut, A. Cozic, Impact of large scale circulation on European summer surface ozone: consequences for modeling, *Atmospheric Environment*, 43(6), Pages 1189-1195, doi:10.1016/j.atmosenv.2008.10.039, 2009.

Valari M. and L. Menut, Does increase in air quality models resolution bring surface ozone concentrations closer to reality?, *J. Atmos. Ocean. Tech.*, doi: 10.1175/2008JTECH A1123.1, 2008.

Vivanco M. G., Palomino I., Vautard R., Bessagnet R., Martin F., Menut L., Jimenez S., Multi-year assessment of photochemical air quality simulation over Spain, *Env. Mod. and Software*, doi:10.1016/j.envsoft.2008.05.004, 2008.

Visschedijk, A.J.H., Zandveld, P.Y.J., and Denier van der Gon, H.A.C.A., High resolution gridded European database for the EU Integrate Project GEMS, *TNO-report* 2007-A-R0233/B.

11.3 EMEP

Andersson-Sköld, Y. and D. Simpson, Comparison of the chemical schemes of the EMEP MSC-W and the IVL photochemical trajectory models, *Atmos. Environ.*, 33(7), 1111-1129, doi:10.1016/S1352-2310(98)00296-9, 1999.

Bergström, R., et al.: Modelling of organic aerosols over Europe (2002–2007) using a volatility basis set (VBS) framework with application of different assumptions regarding the formation of secondary organic aerosol, *Atmos. Chem. Phys.*, 12, 8499-8527, 2012.

Binkowski, F. S., and U. Shankar (1995), The Regional Particulate Matter Model 1. Model description and preliminary results, *J. Geophys. Res.*, 100(D12), 26,191–26,209, doi:10.1029/95JD02093.

Bott, A., A positive definite advection scheme obtained by nonlinear renormalization of the advective fluxes, *Mon. Weather Rev.*, 117(5), 1006-1016, doi:10.1175/1520-0493(1989)117(1006:APDASO)2.0.CO;2, 1989.

Ciarelli, G. et al., Constraining a hybrid volatility basis-set model for aging of wood-burning emissions using smog chamber experiments: a box-model study based on the VBS scheme of the CAMx model (v5.40), *Geosc. Model Devel.*, 2017, 10, 2303-2320.

Denier van der Gon, H. A. C. et al., Particulate emissions from residential wood combustion in Europe – revised estimates and an evaluation, *Atmos. Chem. Phys.*, 2015, 15, 6503-6519.

Dunmore, RE et al., Diesel-related hydrocarbons can dominate gas phase reactive carbon in megacities, *Atmos. Chem. Phys.* 2015, 15, 9983-9996.

Emberson, L., et al., Towards a model of ozone deposition and stomatal uptake over Europe, *EMEP MSC-W Note 6/2000*, Norwegian Meteorological Institute, Norway, 2000.

EMEP Transboundary acidification, eutrophication and ground level ozone in Europe in 2013, *EMEP Status Report 1/2015*, 2015 (available online at http://emep.int/mscw/mscw_publications.html).
Gerber, H. E.: Relative-Humidity Parameterization of the Navy Aerosol Model (NAM), *NRL Report 8956*, Naval Research Laboratory, Washington, DC, 1985.

Jathar, SH et al., Chemical transport model simulations of organic aerosol in southern California: model evaluation and gasoline and diesel source contributions, *Atmos. Chem. Phy*s. 2017, 17, 4305-4318.

Kahnert, M., On the observability of chemical and physical aerosol properties by optical observations: Inverse modelling with variational data assimilation, *Tellus*, doi:10.1111/j.1600-0889.2009.00436.x, 2009.

Kettle, A. J., Andreae, M. O., et al., et al., and et al.: A global data base of sea surface dimethylsulfide (DMS) measurements and a procedure to predict sea surface DMS as a function of latitude, longitude, and month, *Global Biogeochem. Cycles*, 13, 399–444, 1999.

May, AA et al., Gas-particle partitioning of primary organic aerosol emissions: 3. Biomass burning, *J. Geoph. Res.*, 2013, 118, 11327-11338.

Ots, R. et al., Simulating secondary organic aerosol from missing diesel-related intermediate-volatility organic compound emissions during the Clean Air for London (ClearfLo) campaign, *Atmos. Chem. Phys.*, 2016, 16, 6453-6473.

Parrish, D. F. and J. C. Derber, The national meteorological center's spectral statistical interpolation analysis system, *Mon. Weather Rev.*, 120(8), 1747-1763, doi:10.1175/1520-0493(1992)120h1747:TNMCSSi2.0.CO;2, 1992.

Platt, S. M. et al., Secondary organic aerosol formation from gasoline vehicle emissions in a new mobile environmental reaction chamber, *Atmos. Chem. Phys.*, 2013, 13, 9141-9158.

Robinson, A. L. et al., Rethinking Organic Aerosols: Semivolatile Emissions and Photochemical Aging, *Science*, 2007, 315, 1259-1262.

Simpson, D., et al., Characteristics of an ozone deposition module 2: sensitivity analysis, *Water, Air and Soil Poll.*, 143, 123-137, 2003.

Simpson, D., et al., The EMEP MSC-W chemical transport model – technical description, *Atmos. Chem. Phys.*, 12, 7825–7865, 2012.

Tuovinen, J.-P., et al., Testing and improving the EMEP ozone deposition module, *Atmos. Environ.*, 38, 2373-2385, 2004.

Valdebenito B. and Heiberg, First results from comparison of model calculated tropospheric NO2 column with GOME data. *Met.no Note 12/2009*, The Norwegian Meteorological Institute, Oslo, Norway, 2009.

Valdebenito B. and Tsyro, The EMEP data assimilation system: Further development and integrity test results. *Met.no Note 1/2012*, The Norwegian Meteorological Institute. Oslo, Norway, 2012.

Valdebenito B. et al. (2010), The EMEP data assimilation system: Technical description and first results. *Met.no Note 4/2010*, Norwegian Meteorological Institute, Oslo, Norway, 2010.

11.4 EURAD-IM

Ackermann, I. et al., *Atmos. Env.*, 32(17), 2981-2999, 1998.

Baklanov, A. and J.H. Sorenson, *Phys. Chem. Earth* (B), 26, 787-799, 2001.

Bott, A., *Mon. Wea. Rev.,* 117 (5), 1006-1015, 1989.

Binkowski, F.S., Aerosols in Models-3 CMAQ, in: *Science algorithms of the EPA Models-3 Community multiscale air quality (CMAQ) modeling system*, EPA 600/R-99-030, EPA, 1999.

Carn, S.A. et al., Geological Society, London*, Special Publications*, 213, 177-202, 2003.

Eckhardt, S. et al., Atmos. Chem. Phys., 8, 3881-3897, https://doi.org/10.5194/acp-8-3881-2008, 2008.

Elbern, H., A. Strunk, H. Schmidt, and O. Talagrand, *Atmos. Chem. Phys.*, 7, 1-59, 2007.

Friese, E. and A. Ebel, *J. Phys. Chem. A*, 114, 11595-11631, 2010.

Geiger, H., I. Barnes, I. Bejan, T. Benter, and M. Spttler, *Atmos. Environ.*, 37, 1503-1519, 2003.

Guenther, A. B., X. Jiang, C.L. Heald, T. Sakulyanontvittaya, T. Duhl, L.K. Emmons, X. Wang, *Geosci. Model Dev.*, 5, 1471-1492, 2012.

Hass, H., H.J. Jakobs, and M. Memmesheimer, *Met. Atmos. Phys.*, 57, 173-200, 1995.

Holtslag, A.A.M. and F.T.M. Nieuwstadt, *Boundary-Layer Met.*, 36, 201-209, 1986.

Ialongo, I. et al., Atmos. Meas. Tech., 8, 2279-2289, https://doi.org/10.5194/amt-8-2279-2015, 2015.

Kaiser, J.W. et al., *Biogeosciences*, 9, 527-554, 2012.

Kharol, Shailesh K. et al., Atmos. Chem. Phys., 17, 5921-5929, 2017.

Li, Y.P. H. Elbern, K.D. Liu, E. Friese, A. Kiendler-Scharr, Th.F. Mentel, X.S. Wang, A. Wahner, and Y.H. Zhang, *Atmos. Chem. Phys.*, 13, 6289 - 6304, 2013.

Liu, D.C. and J. Nocedal, *Math. Programming*, 45, 503-528, 1989.

McLinden, C. et al., *Nature Geoscience*, 9, 496-500, 2016.

Madronich, S. and G. Weller, *J. Atmos. Chem.*, 10, 289-300, 1990.
McRae, G.J., W.R. Goodin and J.H. Seinfeld, *J. Comp. Phys.*, 45, 1-42, 1982.

Memmesheimer, M. et al., *Int. J. Environm. and Pollution*, 22, (1-2), 108-132, 2004.

Nickovic, S., G. Kallos, A. Papadopoulos, and O. Kakaliagou, A model for prediction of desert dust cycle in the atmosphere, *J. Geophs. Res.*, 106 (D16), 18113-18129, 2001.

Nieradzik, L.P., *Application of a high dimensional model representation on the atmospheric aerosol module MADE of the EURAD-CTM*, Master Thesis, Institut für Geophysik und Meteorologie der Universität zu Köln, 2005.

Nocedal, J., *Math. Comput.*, 35 (151), 773-782, 1980.

Petroff, A. and L. Zhang, *Geosci. Model Dev.*, 3, 753-769, doi: 10.5197/gmd-3-753-2010.

Rabitz, H., O. Alis, J. Shorter, and K. Shim, *J. Math. Chem.*, 25, 197-233, 1999.

Roselle, S.J. and F.S. Binkowski, Cloud Dynamics and Chemistry, in: *Science algorithms of the EPA Models-3 Community multiscale air quality (CMAQ) modeling system*, EPA 600/R-99-030, EPA, 1999.

Sandu, A. and R. Sander, *Atmos. Chem. Phys.*, 6, 187-195, 2006.

Sofiev et al., *Atmos. Chem. Phys*., 15, 8115-81130, 2015.

Sofiev et al., *Atmos. Chem. Phys. Discuss*., https://doi.org/10.5149/acp-2016-1189, in review.

Stockwell, W.R., F. Kirchner, M. Kuhn, and S. Seefeld, *J. Geophys. Res.*, 102 (D22), 25847-25879, 1997.
Tie, X. et al., J. Geophys. Res., 108, D20, 4642, 2003.

Weaver, A. and P. Courtier, Q. *J. R. Meteorol. Soc.*, 127, 1815-1846, 2001.

Zhang, L., J.R. Brook, and R. Vet, *Atmos. Chem. Phys.*, 3, 2067-2082, 2003.

11.5 LOTOS-EUROS

Banzhaf, S., Schaap, M., Kerschbaumer, A., Reimer, E., Stern, R., van der Swaluw, E., and Builtjes, P.: Implementation and evaluation of pH-dependent cloud chemistry and wet deposition in the chemical transport model REM-Calgrid, *Atmos. Environ.*, 49, 378–390, 2012.

Barbu, A., Segers, A., Schaap, M., Heemink, A. and Builtjes, P.J.H., A multi-component data assimilation experiment directed to Sulphur dioxide and sulphate over Europe, *Atmos. Env.*, 43(9), 1622-1631, 2008.

Bieser, J., A. Aulinger, V. Matthias, M. Quante, H.A.C. Denier van der Gon, Vertical emission profiles for Europe based on plume rise calculations,Environmental Pollution, Volume 159, Issue 10, 2011, Pages 2935-2946, doi:10.1016/j.envpol.2011.04.030

Curier, R.L., Timmermans, R., Calabretta-Jongen, S., Eskes H., Segers, A., Swart, D., and Schaap, M., Improving ozone forecasts over Europe by synergistic use of the LOTOS-EUROS chemical transport model and in-situ measurements, *Atmospheric Environment*, Volume 60, Pages 217-226, 2012.

Fécan, F., B. Marticorena, and G. Bergametti (1999). "Parametrization of the increase of the aeolian erosion threshold wind friction velocity due to soil moisture for arid and semi-arid areas". *Annales Geophysicae* 17.1, pp. 149–157. DOI: 10.1007/s00585-999-0149-7.
Ginoux, P., M. Chin, I. Tegen, B. Prospero J.M.and Holben, O. Dubovik, and S.-J. Lin (2001). "Sources and distributions of dust aerosols simulated with the GOCART model". *Journal of Geophysical Research* D: Atmospheres. DOI: 10.1029/2000JD000053.

Guenther, A. B., P. R. Zimmerman, P. C. Harley, R. K. Monson and R. Fall, Isoprene and Monoterpene Emission Rate Variability: Model Evaluations and Sensitivity Analyses, *J. Geophys. Res.*, 98, 1993.

Heinold, B.I., Helmert J., Hellmuth O., Wolke R., Ansmann A., Marticorena B, Laurent B., and Tegen (2007). "Regional modeling of Saharan dust events using LM-MUSCAT: Model description and case studies". *Journal of Geophysical Research* D: Atmospheres. DOI: 10.1029/2006JD007443.

Hendriks, C., R. Kranenburg, J. Kuenen, R. van Gijlswijk, R. Wichink Kruit, A. Segers, H. Denier van der Gon, M. Schaap, The origin of ambient particulate matter concentrations in the Netherlands. *Atmospheric Environment*, 69, p. 289-303, 2013.

Fountoukis, C. and Nenes, A., ISORROPIA II: A Computationally Efficient Aerosol Thermodynamic Equilibrium Model for K+, Ca2+, Mg2+, NH4+, Na+, SO42-, NO3-, Cl-, H2O Aerosols, *Atmos. Chem. Phys.*, 7, 4639–4659, 2007.

Köble R. and G. Seufert, *Novel Maps for Forest Tree Species in Europe*, 2001.

Kuenen, J. J. P., Visschedijk, A. J. H., Jozwicka, M., and Denier van der Gon, H. A. C.: TNO-MACC_II emission inventory; a multi-year (2003–2009) consistent high-resolution European emission inventory for air quality modelling, *Atmos. Chem. Phys.*, 14, 10963-10976, doi:10.5194/acp-14-10963-2014, 2014.

Manders, A. M. M., Builtjes, P. J. H., Curier, L., Denier van der Gon, H. A. C., Hendriks, C., Jonkers, S., Kranenburg, R., Kuenen, J., Segers, A. J., Timmermans, R. M. A., Visschedijk, A., Wichink Kruit, R. J., Van Pul, W. A. J., Sauter, F. J., van der Swaluw, E., Swart, D. P. J., Douros, J., Eskes, H., van Meijgaard, E., van Ulft, B., van Velthoven, P., Banzhaf, S., Mues, A., Stern, R., Fu, G., Lu, S., Heemink, A., van Velzen, N., and Schaap, M.Curriculum Vitae of the LOTOS-EUROS (v2.0) chemistry transport model Geosci. Model Dev. https://doi.org/10.5194/gmd-10-4145-2017, 2017.

Martensson, E. M., Nilsson, E. D., de Leeuw, G., Cohen, L. H., and Hansson, H. C.: Laboratory simulations and parameterization of the primary marine aerosol production, *J. Geophys. Res.*, 108, 4297, 2003.

Marticorena, B. and G. Bergametti (1995). "Modeling the atmospheric dust cycle: 1. Design of a soil-derived dust emission scheme". *Journal of Geophysical Research* 100.D8,p. 16415. DOI: 10.1029/95JD00690.

Schaap, M., van Loon, M., ten Brink, H.M., Dentener, F.D. and Builtjes, P.J.H. (2004b) 'Secondary inorganic aerosol simulations for Europe with special attention to nitrate', *Atmospheric Physical Chemistry*, Vol. 4, pp.857–874.

Schaap, M., F. Sauter, R.M.A. Timmermans, M. Roemer, G. Velders, J. Beck and P.J.H. Builtjes, The LOTOS-EUROS model: description, validation and latest developments, *Int. J. Environment and Pollution*, Vol. 32, No. 2, pp.270&–290, 2008.

Seinfeld, J. H. and Pandis, S. N., Atmospheric Chemistry and Physics: from air pollution to climate change, Wiley-Interscience, Hoboken, N.J., 2006.

Shao, Yaping (2001). "A model for mineral dust emission". *Journal of Geophysical Research*: Atmospheres 106.D17, pp. 20239–20254. DOI: 10.1029/2001JD900171.

Skjoth, C. A., Geels, C., Berge, H., Gyldenkaerne, S., Fagerli, H., Ellermann, T., ... & Hertel, O. (2011). Spatial and temporal variations in ammonia emissions - a freely accessible model code for Europe. Atmospheric Chemistry and Physics, 11(11), 5221-5236.

Solazzo, E.; Bianconi, R.; Vautard, R.; Appel, K.W.; Moran, M.D.; Hogrefe, C.; Bessagnet, B.; Brandt, J.; Christensen, J.H.; Chemel, C. Model Evaluation and Ensemble Modelling of Surface-Level Ozone in Europe and North America in the Context of AQMEII. *Atmos. Environ.*, 2012a.

Solazzo, E.; Bianconi, R.; Pirovano, G.; Matthias, V.; Vautard, R.; Moran, M.D.; Wyat Appel, K.; Bessagnet, B.; Brandt, J.; Christensen, J.H. Operational Model Evaluation for Particulate Matter in Europe and North America in the Context of AQMEII. *Atmos. Environ.*, 2012b.

Stern, R., Builtjes, P., Schaap, M., R. Timmermans, R. Vautard, A. Hodzic, M. Memmesheimer, H. Feldmann, E. Renner R. Wolke and A. Kerschbaumer, A model inter-comparison study focussing on episodes with elevated PM10 concentrations, *Atmos. Environ.*, 42, 4567-4588, 2008.

Zhang, L, Gong, S., Padro, J., Barrie, L., 2001. A size-segregated particle dry deposition scheme for an atmospheric aerosol module. *Atmospheric Environment*, 35(3), Pages 549–560, 2001.

Zobler, L (1986). A World soil file for global climate modelling. *Technical Memorandum NASA-TM-*87802. NASA.

11.6 MATCH

Bergström, J. R., Carbonaceous Aerosol in Europe – *Out of the Woods and into the Blue?*; Department of Chemistry and Molecular Biology, University of Gothenburg, SE-412 96 Göteborg, Sweden; summary available online at: , 2015.

Bergström, R., Denier van der Gon, H.A.C., Prévôt, A.S.H., Yttri, K.E., Simpson, D., Modelling of organic aerosols over Europe (2002–2007) using a volatility basis set (VBS) framework: application of different assumptions regarding the formation of secondary organic aerosol, *Atmos. Chem. Phys.*, 12, 8499-8527, 2012.

Burridge, D. M. and Gadd, A. J., The meteorological office operational 10-level numerical weather predictions model. *Sc.*, *Paper*, No 34, Meteor. Office, London Road. Bracknell, Birkshire RG12 2sz, England, 1-39, 1977.

Carter, W.P.L, Condensed atmospheric photo oxidation mechanism for isoprene, *Atmos. Env.* 30, 4275-4290, 1996.

Denier van der Gon, H. A. C., Kuenen, J. J. P. and Visschedijk, A. J. H.: personal communication, 2015a.

Denier van der Gon, H. A. C., Bergström, R., Fountoukis, C., Johansson, C., Pandis, S. N., Simpson, D., and Visschedijk, A. J. H.: Particulate emissions from residential wood combustion in Europe – revised estimates and an evaluation, *Atmos. Chem. Phys.*, 15, 6503-6519, doi:10.5194/acp-15-6503-2015, 2015b.

Heimann, M. and Keeling, C.D., A three-dimensional model of CO2 tramsport based on observed winds. Model description and simulated trace experiment. In *Aspects of Climate Variability in the Pacific and Western Americas* (ed. D.H Peterson). American Geophysical Union, Washington, DC, pp. 237-275, 1989.

Hodzic, A., Kasibhatla, P. S., Jo, D. S., Cappa, C. D., Jimenez, J. L., Madronich, S., and Park, R. J.: Rethinking the global secondary organic aerosol (SOA) budget: stronger production, faster removal, shorter lifetime, *Atmos. Chem. Phys.*, 16, 7917-7941, doi:10.5194/acp-16-7917-2016, 2016.

Holtslag, A. A. M., Boville. B. A.: Moeng, V.-H., Invited paper ECMWF, Reading UK, 16-18 September, 1991.

Holtslag. A.A.M., Meigaard, E. van and De Rooy, W.C., A comparison of boundary layer diffusion schemes in unstable conditions over land. *Boundary Layer Met.*, 76, 69-95, 1995.

Kahnert, M., Variational data analysis of aerosol species in a regional CTM: Background error covariance constraint and aerosol optical observations operators, *Tellus*, 60B, 753-770, 2008.

Kuenen, J. J. P., Visschedijk, A. J. H., Jozwicka, M., and Denier van der Gon, H. A. C.: *Atmos. Chem. Phys.*, 14, 10963-10976, doi:10.5194/acp-14-10963-2014, 2014.

Lane, T. E., Donahue, N. M., and Pandis, S. N.: Effect of NOx on secondary organic aerosol concentrations, *Environ. Sci. Technol.,* 42, 6022–6027, doi:10.1021/es703225a, 2008.

Langner, J., Bergström, R. and Pleijel, K., European scale modeling of sulphur, oxidized nitrogen and photochemical oxidants. Model dependent development av evaluation for the 1994 growing season. *SMHI report*, RMK No. 82, Swedish Met. And Hydrol. Inst., Norrköping, Sweden, 1998.

Ots, R., Young, D. E., Vieno, M., Xu, L., Dunmore, R. E., Allan, J. D., Coe, H., Williams, L. R., Herndon, S. C., Ng, N. L., Hamilton, J. F., Bergström, R., Di Marco, C., Nemitz, E., Mackenzie, I. A., Kuenen, J. J. P., Green, D. C., Reis, S., and Heal, M. R.: Simulating secondary organic aerosol from missing diesel-related intermediate-volatility organic compound emissions during the Clean Air for London (ClearfLo) campaign, *Atmos. Chem. Phys.*, 16, 6453-6473, doi:10.5194/acp-16-6453-2016, 2016.

Parish, D.F. and Derber, J.C., The national Meteorological Center's spectral statistical interpolation analysis system. *Mon. Wea. Rev.* 120, 1747-1763, 1992.

Robertson, L., Langner, J. and Engardt, M., An Eulerian limited-area atmospheric transport model, *J. Appl. Met.* 38, 190-210, 1999.

Simpson, D.: Biogenic emissions in Europe 2: Implications for ozone control strategies, *J. Geophys. Res.*, 100, 22891–22906, 1995.

Simpson, D., Benedictow, A., Berge, H., Bergström, R., Emberson, L. D., Fagerli, H., Flechard, C. R., Hayman, G. D., Gauss, M., Jonson, J. E., Jenkin, M. E., Nyíri, A., Richter, C., Semeena, V. S., Tsyro, S., Tuovinen, J.-P., Valdebenito, Á., and Wind, P., The EMEP MSC-W chemical transport model – technical description, *Atmos. Chem. Phys.*, 12, 7825-7865, doi:10.5194/acp-12-7825-2012, 2012.

Sofiev, M., J. Soares, M. Prank, G. de Leeuw, and J. Kukkonen, A regional to global model of emission and transport of sea salt particles in the atmosphere, *J. Geophys. Res.*, 116, D21302, doi:10.1029/2010JD014713. 2011.

van Ulden, A.P and Holtslag, A.A.M., Estimation of atmospheric boundary layer parameters for diffusion applications, *J. Climate. Appl. Met.*, 24, 1196-1207, 1985.

Walter, C., Freitas, S. R., Kottmeier, C., Kraut, I., Rieger, D., Vogel, H., and Vogel, B.: The importance of plume rise on the concentrations and atmospheric impacts of biomass burning aerosol, *Atmos. Chem. Phys.*, 16, 9201-9219, https://doi.org/10.5194/acp-16-9201-2016, 2016.

Zilitinkevich, S. and Mironov, D.V., A multi-limit formulation for the equilibrium depth of a stable stratified boundary layer. Max-Planck-Institute for Meteorology. *Report* No. 185, ISSN 0397-1060, 30 pp., 1996.

11.7 MOCAGE

Bechtold, P., E. Bazile, F. Guichard, P. Mascart and E. Richard, A mass flux convection scheme for regional and global models, *Quart. J. Roy. Meteor. Soc.*, 127, 869-886, 2001.

Giorgi, F. and W. L. Chameides, Rainout Lifetimes of Highly Soluble Aerosols and Gases as Inferred From Simulations With a General Circulation Model, *J. Geophys. Res.*, 91(D13), 367-376, 1986.

Guth, J., Josse, B., Marécal, V., Joly, M., and Hamer, P.: First implementation of secondary inorganic aerosols in the MOCAGE version R2.15.0 chemistry transport model, *Geosci. Model Dev.*, 9, 137-160, doi:10.5194/gmd-9-137-2016, 2016.

Josse B., Simon P. and V.-H. Peuch, Rn-222 global simulations with the multiscale CTM MOCAGE, *Tellus*, 56B, 339-356, 2004.

Lagarde, T., Piacentini, A. and O. Thual, A new representation of data assimilation methods: the PALM flow charting approach, *Q.J.R.M.S.*, 127, 189-207, 2001.

Lahoz, W.A., et al, The Assimilation of Envisat data (ASSET) project, *Atmos. Chem. Phys.*, 7, 1773-1796, 2007.

Lefèvre, F., Brasseur, G. P., Folkins, I., Smith, A. K. and P. Simon, Chemistry of the 1991-1992 stratospheric winter: three-dimensional model simulations, *J. Geophys. Res.*, 99 (D4), 8183-8195, 2004.

Louis J.F., A parametric model of vertical eddy fluxes in the atmosphere, *B. Layer Meteor.*, 17, 197-202, 1979.

Madronich S., Photodissociation in the atmosphere, 1. Actinic flux and the effects of ground reflections and clouds, *J. Geophys. Res.*, 92, 9740-9752, 1987.

Mari, C., Jacob, D.J. and Betchold,P., Transport and scavenging of soluble gases in a deep convective cloud, *J. Geophys. Res.*, 105, D17, 22, 255–22267, 2000.

Martet, M., V.-H. Peuch, B. Laurent, B. Marticorena and G. Bergametti, evaluation of long-range transport and deposition of desert dust with the CTM Mocage, *Tellus*, 61B, 449-463, 2009.

Ménégoz, M., D. Salas y Melia, M. Legrand, H. Teyssèdre, M. Michou, V.-H. Peuch, M. Martet, B. Josse and I. Etchevers-Dombrowski, Equilibrium of sinks and sources of sulphate over Europe: comparison between a six-year simulation and EMEP observations, *Atmos. Chem. Phys.*, 9, 4505-4519, 2009.

Michou M., P. Laville, D. Serça, A. Fotiadi, P. Bouchou and V.-H. Peuch, Measured and modeled dry deposition velocities over the ESCOMPTE area, *Atmos. Res.*, 74 (1-4), 89-116, 2004.

Nho-Kim, E.-Y., V.-H. Peuch and S. N. Oh, Estimation of the global distribution of Black Carbon aerosols with MOCAGE, *J. Korean Meteor. Soc.*, 41(4), 587-598, 2005.

Nho-Kim, E.-Y., M. Michou and V.-H. Peuch, Parameterization of size dependent particle dry deposition velocities for global modeling, *Atmos. Env.*, 38 (13), 1933-1942, 2004.

Noilhan, J. and S. Planton, A simple parameterization of land surface processes for meteorological models, *Mon. Wea. Rev.*, 117, 536-549, 1989.

Rouil, L., et al, PREV'AIR: an operational forecasting and mapping system for air quality in Europe, *Bull. Am. Meteor. Soc.*, 90(1), 73-83, doi:10.1175/2008BAMS2390.1, 2008.

Sič, B., L. El Amraoui, V. Marécal, B. Josse, J. Arteta, J. Guth, M. Joly, and P. Hamer, Modelling of primary aerosols in the chemical transport model MOCAGE: development and evaluation of aerosol physical parameterizations, *Geosci. Mod. Dev.*, 8, 381-408, 2015.

Stockwell, W.R. et al., A new mechanism for regional atmospheric chemistry modelling, *J. Geophys. Res.*, 102, 25847-25879, 1997.

Wesely, M. L., Parameterization of surface resistance to gaseous dry deposition in regional numerical models, *Atmos. Env.*, 16, 1293-1304, 1989.

Williamson, D. L. and P. J. Rash, Two-dimensional semi-lagrangian transport with shape-preserving interpolation, *Mon. Wea. Rev.*, 117, 102-129, 1989.

11.8 SILAM

Bieser, J., A. Aulinger, V. Matthias, M. Quante, H.A.C. Denier van der Gon, Vertical emission profiles for Europe based on plume rise calculations, *Environmental Pollution*, Volume 159, Issue 10, 2011, Pages 2935-2946, doi:10.1016/j.envpol.2011.04.030.

Damski, J., Thölix, L., Backman, L., Taalas, P., Kulmala, M., 2007. FinROSE: middle atmospheric chemistry transport model. *Boreal Environ. Res.* 12, 535–550.

Donahue, N. M., a. L. Robinson, C. O. Stanier, and S. N. Pandis, Coupled partitioning, dilution, and chemical aging of semivolatile organics, *Environmental Science and Technology*, 40 (8), 2635-2643, doi:10.1021/es052297c, 2006.

Gery, M., G. Whitten, J. Killus, and M. Dodge, A photochemical kinetics mechanism for urban and regional scale computer modeling, *Journal of Geophysical Research*, 94, D10, pp 12925-12956, 1989.

Jalkanen, J.-P. et al. A modelling system for the exhaust emissions of marine traffic and its application in the Baltic Sea area. *Atmos. Chem. Phys.* Discuss. 9, 15339-15373 (2009).

Kouznetsov, R., Sofiev, M. (2012) A methodology for evaluation of vertical dispersion and dry deposition of atmospheric aerosols. *JGR*,117, DOI: 10.1029/2011JD016366.

Kukkonen J, Olsson T, Schultz D, Baklanov A, Klein T, Miranda A, Monteiro A, Hirtl M, Tarvainen V, Boy M, Peuch V, Poupkou A, Kioutsioukis I, Finardi S, Sofiev M, Sokhi R, Lehtinen K, Karatzas K, San José R, Astitha M, Kallos G, Schaap M, Reimer E, Jakobs H, Eben K. (2012) A review of operational, regional-scale, chemical weather forecasting models in Europe. *Atmos. Chem. Phys.*, 12, 1-87, doi:10.5194/acp-12-1-2012.

Poupkou, A., Giannaros, T., Markakis, K., Kioutsioukis, I., Curci, G., Melas, D., Zerefos, C., A model for European Biogenic Volatile Organic Compound emissions, 2010: Software development and first validation, *Env. Model. & Software*, 25, 1845-1856.

Lane, T. E., N. M. Donahue, and S. N. Pandis, Simulating secondary organic aerosol formation using the volatility basis-set approach in a chemical transport model, *Atmospheric Environment*, 42 (32), 7439-7451, doi:10.1016/j.atmosenv.2008.06.026, 2008.

Prank, M., Vira, J., Ots, R., Sofiev, M., (2016), Evaluation of organic aerosol and its precursors in the SILAM model, Proceedings of the 35th International Technical Meeting on Air Pollution Modelling and its Application, 3-7 October 2016, Chania, Crete, Greece.

Price, C.G., J.E. Penner and M.J. Prather, 1997, NOx from lightning, Part I: Global distribution based on lightning physics, J.
Geophys. Res., 102:D5, 5929-5941

Robinson, A. L., N. M. Donahue, M. K. Shrivastava, E. a. Weitkamp, A. M. Sage, A. P. Grieshop, T. E. Lane, J. R. Pierce, and S. N. Pandis, Rethinking Organic Aerosols: Semivolatile Emissions and Photochemical Aging, *Science*, 315, 1259-1262, doi:10. 1126/science.1133061, 2007.

Shrivastava, M., J. Fast, R. Easter, W. I. Gustafson, R. a. Zaveri, J. L. Jimenez, P. Saide, and A. Hodzic, Modeling organic aerosols in a megacity: Comparison of simple and complex representations of the volatility basis set approach, *Atmospheric Chemistry and Physics*, 11 (13), 6639-6662, doi:10.5194/acp-11-6639-2011, 2011.

Shrivastava, M. K., T. E. Lane, N. M. Donahue, S. N. Pandis, and A. L. Robinson, Effects of gas particle partitioning and aging of primary emissions on urban and regional organic aerosol concentrations, *Journal of Geophysical Research Atmospheres*, 113 (18), 1-16, doi:10.1029/2007JD009735, 2008.

Sofiev, M. (2002), Extended resistance analogy for construction of the vertical diffusion scheme for dispersion models, *J. Geophys. Res.*, 107(D12), doi: 10.1029/2001JD001233, 2002.

Sofiev, M., (2016) On impact of transport conditions on variability of the seasonal pollen index. *Aerobiologia,* DOI: 10.1007/s10453-016-9459-x.

Sofiev, M., Berger, U., Prank, M., Vira, J., Arteta, J., Belmonte, J., Bergmann, K.-C., Chéroux, F., Elbern, H., Friese, E., Galan, C., Gehrig, R., Khvorostyanov, D., Kranenburg, R., Kumar, U., Marécal, V., Meleux, F., Menut, L., Pessi, A.-M., Robertson, L., Ritenberga, O., Rodinkova, V., Saarto, A., Segers, A., Severova, E., Sauliene, I., Siljamo, P., Steensen, B. M., Teinemaa, E., Thibaudon, M., and Peuch, V.-H. (2015) MACC regional multi-model ensemble simulations of birch pollen dispersion in Europe, *Atmos. Chem. Phys*., 15, 8115-8130, doi :10.5194/acp-15-8115-2015.

Sofiev, M., Vira, J., Kouznetsov, R., Prank, M., Soares, J., Genikhovich, E. (2015) Construction of an Eulerian atmospheric dispersion model based on the advection algorithm of M.Galperin: dynamic cores v.4 and 5 of SILAM v.5.5, *Geosci. Model Developm.* Discuss., 8, 2905-2947, doi:10.5194/gmdd-8-2905-2015.

Vira, J., Sofiev, M. (2012) On variational data assimilation for estimating the model initial conditions and emission fluxes for the short-term forecasting of SOx concentrations. *Atmosph. Environ.*, 46, pp.318-328, doi:10.1016/j.atmosenv.2011.09.066.

Vira, J., Sofiev, M. (2015) Assimilation of surface NO2 and O3 observations into the SILAM chemistry transport model, *Geosci. Model Dev.*, 8, 191–203, , doi:10.5194/gmd-8-191-2015.

Wang, S., 2012: *J. Hydrometeor.,* 13, 239–254,

Yarwood, G., S. Rao, M. Yocke, and G. Whitten, Updates to the carbon bond chemical mechanism: CB05. Final Report, Tech. rep., RT-04-00675, U.S. EPA, 2005.

11.9 DEHM

Bergström, R., Denier van der Gon, H. A. C., Prévôt, A. S. H., Yttri, K. E., and Simpson, D., 2012. Modelling of organic aerosols over Europe (2002–2007) using a volatility basis set (VBS) framework: application of different assumptions regarding the formation of secondary organic aerosol, *Atmos. Chem. Phys.*, 12, 8499-8527, doi:10.5194/acp-12-8499-2012.

Christensen, J. H., 1997. The Danish Eulerian Hemispheric Model – a three-dimensional air pollution model used for the Arctic, *Atmospheric Environment*, 31, 4169–4191.

Dabdub, D., Seinfeld, J.H., 1994. Numerical advective schemes used in air quality models - sequential and parallel implementation. *Atmospheric Environment*, 28, 3369-3385.

Emberson, L., Simpson, D., Tuovinen, J.-P., Ashmore, M.R., Cambridge, H.M., 2000. Towards a Model of Ozone Deposition and Stomatal Uptake over Europe. *EMEP MSC-W Note 6/2000*.

Forester, C.K., 1977. Higher order monotonic convective difference schemes. *Journal of Computational Physics* 23, 1-22.

Frohn, L., 2004. A study of long-term high-resolution air pollution modelling, *PhD. thesis*, National Environmental Research Institute.

Frydendall, J., Brandt, J., Christensen, J. H., 2009. Implementation and testing of a simple data assimilation algorithm in the regional air pollution forecast model, DEOM. *Atmos. Chem. Phys.*, 9, 5475-5488.

Heidam, N. Z., Christensen, J., Wahlin, P., and Skov, H., 2004. Arctic atmospheric contaminants in NE Greenland: levels, variations, origins, transport, transformations and trends 1990-2001: *Science of the Total Environment*, 331, 5-28.

Heidam, N. Z., Wahlin, P., and Christensen, J. H., 1999. Tropospheric gases and aerosols in northeast Greenland: *Journal of the Atmospheric Sciences*, 56, 261-278.

Hertel, O., Christensen, J., Runge, E., Asman, W. A. H.,Berkowicz, R., Hovmand, M. and Hov, O., 1995. Development and testing of a new variable scale air pollution modeI-ACDEP. *Atmospheric Environment* 29, 1267- 1290.

Jonson, J. E., A. Kylling, T. Berntsen, I. S. A. Isaksen, C. S. Zerefos and K. Kourtidis, 2000. Chemical effects of uv fluctuation inferred from total ozone and tropospheric aerosol variations, *J. Geophys. Res.*, 105, 14561-14574.

Kahnert, M., 2008. Variational data analysis of aerosol species in a regional CTM: background error covariance constraint and aerosol optical observation operators. *Tellus B,* 60, 753–770. https://doi.org/10.1111/j.1600-0889.2008.00377.x.

Lambert, J.D., 1991. *Numerical Methods for Ordinary Differential Systems: The Initial Value Problem*. John Wiley & Sons, Chichesters.

Lane, T. E., Donahue, N. M., and Pandis, S. N., 2008, Simulating secondary organic aerosol formation using the volatility basis-set approach in a chemical transport model, *Atmospheric Environment*, 42, 7439–7451, doi:10.1016/j.atmosenv.2008.06.026.

Pepper, D.W., Kern, C.D., Long, P.E., 1979. Modeling the dispersion of atmospheric pollution using cubic-splines and Chapeau functions. *Atmospheric Environment* 13, 223-237.

Seinfeld, J. H., 1986. *Atmospheric Chemistry and Physics of Air Pollution*. Wiley, New York.

Schultz M., et al., 2007, RETRO report on emission data sets and methodologies for estimating emissions, Workpackage 1, Deliverable D1–6, EU-Contract No. EVK2-CT-2002-00170.

Silver, J.D., Brandt, J., Hvidberg, M., Frydendall, J., Christensen, J.H., 2013. Assimilation of OMI NO2 retrievals into the limited-area chemistry-transport model DEHM (V2009.0) with a 3-D OI algorithm. *Geoscientific Model Development* 6, 1–16. https://doi.org/10.5194/gmd-6-1-2013

Silver, J. D., Christensen, J. H., Kahnert, M., Robertson, L., Rayner, P. J., and Brandt. J., 2016. Multi-species chemical data assimilation with the Danish Eulerian hemispheric model: system description and verification, *Journal of Atmospheric Chemistry*, 73: 261-302.

Simpson, D., Fagerli, H., Jonson, J.E., Tsyro, S., Wind, P., Tuovinen J-, P., 2003. Transboundary Acidification, Eutrophication and Ground Level Ozone in Europe, PART I, *Unified EMEP Model Description*, 104 pp.

Soares, J., Sofiev, M., Geels, C., Christensen, J. H., Andersson, C., Tsyro, S., and Langner, J., 2016. Impact of climate change on the production and transport of sea salt aerosol on European seas, *Atmos. Chem. Phys*., 16, 13081-13104, doi:10.5194/acp-16-13081-2016.

Strand, A., Hov, O., 1994. A 2-Dimensional global study of tropospheric ozone production. *Journal of Geophysical Research-Atmospheres* 99, 22877-22895.

Zare, A., J. H. Christensen, P. Irannejad and J. Brandt, 2012. Evaluation of two isoprene emission models for using in a long-range air pollution model. *Atmos. Chem. Phys*., 12, pp. 7399-7412, 2012. www.atmos-chem-phys.net/12/7399/2012/. doi:10.5194/acp-12-7399-2012.

Zare, A., J. H. Christensen, A. Gross, P. Irannejad, M. Glasius and J. Brandt, 2014. Quantifying the contributions of natural emissions to ozone and total fine PM concentrations in the Northern Hemisphere. *Atmos. Chem. Phys*. Vol. 14, pp. 2735-2756, 2014, www.atmos-chem-phys.net/14/2735/2014/. doi:10.5194/acp-14-2735-2014.

Schultz M., et al. (2007), RETRO report on emission data sets and methodologies for estimating emissions, Workpackage 1, Deliverable D1–6, EU-Contract No. EVK2-CT-2002–00170.

11.10 GEM-AQ

Bouttier F. and Courtier P., 1999. ECMWF Lecture Notes on Data Assimilation ().

Côté, J., Desmarais, J.-G., Gravel, S., Méthot, A., Patoine, A., Roch, M., and Staniforth, A.: The operational CMC–MRB Global Environmental Multiscale (GEM) Model. Part II: Results, *Mon. Wea. Rev.*, 126, 1397–1418, 1998a.

Côté, J., Gravel, S., Méthot, A., Patoine, A., Roch, M., and Staniforth, A.: The operational CMC–MRB Global Environmental Multiscale (GEM) Model. Part I: Design considerations and formulation, *Mon. Wea. Rev.*, 126, 1373–1395, 1998b.

Glatthor, N., Höpfner, M., Semeniuk, K., Lupu, A., Palmer, P. I., McConnell, J. C., Kaminski, J. W., von Clarmann, T., Stiller, G. P., Funke, B., Kellmann, S., Linden, A., and Wiegele, A.: The Australian bushfires of February 2009: MIPAS observations and GEM-AQ model results, Atmos. Chem. Phys., 13, 1637-1658, doi:10.5194/acp-13-1637-2013, 2013.

Gong, S. L., Barrie, L. A., Blanchet, J.-P., von Salzen, K., Lohmann, U., Lesins, G., Spacek, L., Zhang, L. M., Girard, E., Lin, H., Leaitch, R., Leighton, H., Chylek, P., and Huang, P.: Canadian Aerosol Module: A size-segregated simulation of atmospheric aerosol processes for climate and air quality models, 1. Module development*, J. Geophys. Res.*, 108, 4007, doi: 10.1029/2001JD002002, 2003a.

Gong S.L., A parameterization of sea-salt aerosol source function for sub and super-micron particles, *Glob. Biogeochem. Cycles*, 17, p. 1097, 2003b.

Hollingsworth, A. and Lönnberg, P.: The statistical structure of short-range forecast errors as determined from radiosonde data, Part I. The wind field, *Tellus*, 38, 111–136, 1986.

Kain, J. and J. Fritsch: *J. Atmos. Sci.,* **47**, 2784–2802, doi: 10.1175/1520-0469(1990)047<2784:AODEPM>2.0.CO;2, 1990.

Kaminski, J. W., Neary, L., Struzewska, J., McConnell, J. C., Lupu, A., Jarosz, J., Toyota, K., Gong, S. L., Côté, J., Liu, X., Chance, K., and Richter, A.: GEM-AQ, an on-line global multiscale chemical weather modelling system: model description and evaluation of gas phase chemistry processes, *Atmos. Chem. Phys.*, 8, 3255-3281, doi:10.5194/acp-8-3255-2008, 2008.

Lupu, A., Kaminski, J. W., Neary, L., McConnell, J. C., Toyota, K., Rinsland, C. P., Bernath, P. F., Walker, K. A., Boone, C. D., Nagahama, Y., and Suzuki, K.: Hydrogen cyanide in the upper troposphere: GEM-AQ simulation and comparison with ACE-FTS observations, Atmos. Chem. Phys., 9, 4301-4313, doi:10.5194/acp-9-4301-2009, 2009.

Lurmann, F. W., Lloyd, A. C., and Atkinson, R.: A chemical mechanism for use in long-range transport/acid deposition computer modeling, *J. Geophys. Res.*, 91, 10 905–10 936, 1986.

Marticorena, B. and G. Bergametti, G., Modeling the atmospheric dust cycle: 1. Design of a soil-derived dust emission scheme, *J. Geophys. Res.*, 100, D8, 10.1029/95JD00690, 16415 - 16430, 1995.
Monahan E.C., D.E. Spiel, K.L. Davidson, A model of marine aerosol generation via whitecaps and wave disruption, E.C. Monahan, G. Mac Niocaill (Eds.), *Oceanic Whitecaps*, D. Reidel, Norwell, Massachusetts (1986), pp. 167–174.

Mozurkewich M. 1993. The dissociation constant of ammonium nitrate and its dependence on temperature, relative humidity and particle size**.** *Atmospheric Environment*, 27A (1993), pp. 261-270

SEC(2011) 208 final http://ec.europa.eu/environment/air/quality/legislation/pdf/sec_2011_0208, Establishing guidelines for demonstration and subtraction of exceedances attributable to natural sources under the Directive 2008/50/EC on ambient air quality and cleaner air for Europe

Slinn, W. G. N. 1977. Some approximations for the wet and dry removal of particles and gases from the atmosphere. *J. Water Air Soil Pollut*. 7,5 13-543.

Sofiev, M., Siljamo, P., Ranta, H., Linkosalo, T., Jaeger, S., Rasmussen, a, … Kukkonen, J. (2012). A numerical model of birch pollen emission and dispersion in the atmosphere. Description of the emission module. *International Journal of Biometeorology*. doi:10.1007/s00484-012-0532-z

Sofiev, M., Ritenberga, O., Albertini, R., Arteta, J., Belmonte, J., Bonini, M., Celenk, S., Damialis, A., Douros, J., Elbern, H., Friese, E., Galan, C., Gilles, O., Hrga, I., Kouznetsov, R., Krajsek, K., Parmentier, J., Plu, M., Prank, M., Robertson, L., Steensen, B. M., Thibaudon, M., Segers, A., Stepanovich, B., Valdebenito, A. M., Vira, J., and Vokou, D.: Multi-model ensemble simulations of olive pollen distribution in Europe in 2014, *Atmos. Chem. Phys. Discuss.*, https://doi.org/10.5194/acp-2016-1189, in review, 2017.

Struzewska, J., Zdunek, M., Kaminski, J. W., Łobocki, L., Porebska, M., Jefimow, M., and Gawuc, L.: Evaluation of the GEM-AQ model in the context of the AQMEII Phase 1 project, *Atmos. Chem. Phys.*, 15, 3971-3990, doi:10.5194/acp-15-3971-2015, 2015.

Venkatram, A., Karamchandani, P. K., and Misra, P. K.: Testing a comprehensive acid deposition model, *Atmos. Environ.*, 22, 737–747, 1988.

Wesely, M. L.: Parameterization of surface resistances to gaseous dry deposition in regional-scale numerical models, *Atmos. Environ.*, 23, 1293–1304, 1989.

Yeh, K.-S., Côté, J., Gravel, S., Méthot, A., Patoine, A., Roch, M., and Staniforth, A.: The CMC–MRB Global Environmental Multiscale (GEM) Model. Part III: Nonhydrostatic Formulation, *Mon. Wea. Rev.*, 130, 339–356, 2002.

Zhang, L., Moran, M. D., Makar, P. A., Brook, J. R., and Gong, S.: Modelling gaseous dry deposition in AURAMS: a unified regional air-quality modelling system, *Atmos. Environ.*, 36, 537– 560, 2002.